European Journal of Medicinal Chemistry 244 (2022) 114839

Contents lists available at ScienceDirect

European Journal of Medicinal Chemistry

journal homepage: www.elsevier.com/locate/ejmech

Research paper

Design, synthesis and anticancer evaluation of novel Se-NSAID hybrid molecules: Identification of a Se-indomethacin analog as a potential therapeutic for breast cancer

Sandra Ramos-Inza [a,b], Ignacio Encío [b,c], Asif Raza [d], Arun K. Sharma [d,**], Carmen Sanmartín [a,b,***], Daniel Plano [a,b,*]

[a] Department of Pharmaceutical Technology and Chemistry, University of Navarra, Irunlarrea 1, E-31008, Pamplona, Spain
[b] Instituto de Investigación Sanitaria de Navarra (IdiSNA), Irunlarrea 3, E-31008, Pamplona, Spain
[c] Department of Health Sciences, Public University of Navarra, Avda. Barañain s/n, E-31008, Pamplona, Spain
[d] Department of Pharmacology, Penn State Hershey Cancer Institute, CH72, Penn State, USA

ARTICLE INFO

Keywords:
Selenium
Selenoester
NSAID
Cytotoxicity
Apoptosis

ABSTRACT

A total of twenty-five novel carboxylic acid, methylester, methylamide or cyano nonsteroidal anti-inflammatory drug (NSAID) derivatives incorporating Se in the chemical form of selenoester were reported. Twenty Se-NSAID analogs exhibited an increase in cytotoxic potency compared with parent NSAID scaffolds (aspirin, salicylic acid, naproxen, indomethacin and ketoprofen). Top five analogs were selected to further study their cytotoxicity in a larger panel of cancer cells and were also submitted to the DTP program of the NCI's panel of 60 cancer cell lines. Compounds **4a** and **4d** stood out with IC_{50} values below 10 μM in several cancer cells along with a selectivity index higher than 5 in breast cancer cells. Remarkably, analog **4d** was found to inhibit cell growth notably in two breast cancer cell lines by inducing apoptosis, and to be metabolized to release the parent NSAID along with the Se fragment. Taken together, our results show that Se-NSAID analog **4d** could be a potential chemotherapeutic drug for breast cancer.

1. Introduction

Inflammation is highly related to cancer and plays a key role in the development and progression of the disease. Thus, targeting inflammation could be a suitable strategy for the prevention and treatment of cancer [1]. In this context, although nonsteroidal anti-inflammatory drugs (NSAIDs) have been traditionally known for their analgesic, anti-inflammatory and antipyretic effects [2], in recent years several epidemiological, preclinical, and clinical studies support their chemopreventive and chemotherapeutic potential use for cancer treatment [3–17]. Remarkably, numerous systematic reviews and meta-analyses to date suggest that NSAIDs could be associated with a reduced risk of breast cancer, particularly aspirin (ASA) [18–25]. Recently, ASA was shown to have a potential preventive effect especially in hormone receptor positive tumors or in situ breast tumors in postmenopausal women [8,21]. Likewise, another recent meta-analysis revealed that ASA administration might reduce the risk of breast cancer specific death, all-cause mortality, and the risk of recurrence and metastasis [22]. Another clinical trial further reported the regular use of ASA for reducing the risk of breast cancer [26], and furthermore, a study suggested that the reduction in risk of breast cancer occurred with a low dose of ASA among women with the hormone receptor-positive/human epidermal growth factor receptor 2 (HER2)-negative subtype [27]. NSAID use was also associated with a decreased risk of invasive breast cancer in menopausal hormonal therapy users [28].

The primary mechanism of action responsible for the therapeutic activity of NSAIDs is the inhibition of cyclooxygenase-1 and -2 (COX-1 and -2) and the suppression of prostaglandin synthesis [29]. Interestingly, overexpression of COX-2 has been detected in ~40% of cases of human breast carcinoma as well as in preinvasive ductal carcinoma in

* Corresponding author. Department of Pharmaceutical Technology and Chemistry, University of Navarra, Irunlarrea 1, E-31008, Pamplona, Spain.
** Corresponding author. Department of Pharmacology, Penn State College of Medicine, Penn State Cancer Institute, CH72, Penn State Milton S. Hershey Medical Center, 500 University Drive, Hershey, PA, 17033, USA.
*** Corresponding author. Department of Pharmaceutical Technology and Chemistry, University of Navarra, Irunlarrea 1, E-31008, Pamplona, Spain.
E-mail addresses: asharma1@pennstatehealth.psu.edu (A.K. Sharma), sanmartin@unav.es (C. Sanmartín), dplano@unav.es (D. Plano).

https://doi.org/10.1016/j.ejmech.2022.114839
Received 19 July 2022; Received in revised form 4 October 2022; Accepted 7 October 2022
Available online 13 October 2022

situ lesions [30]. In addition, numerous evidences revealed that NSAIDs could also exert their chemotherapeutic activity through COX-independent mechanisms, such as increasing the expression of caspase-3 by the downregulation of AP-2α [31]; regulation of the Wnt pathway [32,33]; induction of apoptosis [34,35]; inhibition of human high-mobility group A2 (HMGA2) [36] and mammalian neuraminidase-1 (Neu-1) [37]; induction of endoplasmic reticulum stress to activate death receptor signaling and BID protein [38]; and regulation of autophagy [39], among others. Furthermore, several efforts have been made to modify NSAID scaffolds to minimize the side effects related to COX inhibition such as gastrointestinal [40] and cardiovascular [41] risks associated with their prolonged use, as well as to develop more effective analogs with new mechanisms of action. In this regard, hydrogen sulfide- (HS) and nitric oxide- (NO) releasing NSAIDs, formed from the combination of these reactive species with NSAIDs, showed a significant reduction of gastric side effects, along with greater antiproliferative effects [42]. The diethylphosphate analogs of nitrate NO-NSAIDs, named phospho-NSAIDs, have also been widely studied and characterized, and have been found to have preclinical chemotherapeutic effect [43]. For instance, HS-ASA suppressed the growth of estrogen receptor negative breast cancer cells by inducing G0/G1 arrest and apoptosis, downregulating the expression of nuclear factor-kappaB (NF-κB) and the thioredoxin reductase (TrxR) activity, and increasing the levels of reactive oxygen species (ROS) [44]. Another ASA derivative, NO-ASA, showed growth inhibition both *in vitro* and *in vivo* associated with the inhibition of the NF-κB signaling pathway in the same type of cells [45]. Likewise, phosphosulindac (OXT-328) induced apoptosis and reduced cell proliferation by suppressing the Wnt/β-catenin signaling in breast cancer stem cells [46].

Another appealing strategy to develop new analogs is the inclusion of selenium (Se) in the structure of NSAIDs. The anticancer properties of Se, mainly at supranutritional levels of supplementation, have been widely reported [47]. Besides, Se supplementation alongside traditional therapies was found to increase the efficacy of anticancer drugs, limit the associated side effects and improve the general conditions of the patients [47]. Furthermore, compounds containing Se have been demonstrated to exert potent anticancer activity in several xenograft models [48–50]. Selenocompounds display their anticancer activity mainly through the regulation of oxidative stress, involvement in angiogenesis [51] and induction of apoptosis [52]. In addition, selenocompounds have been proven to have a potential synergistic effect in combination with other chemotherapeutic agents [53,54] including NSAIDs [55].

The efficacy of selenocompounds as anticancer drugs is correlated with the dose, the metabolic routes involved and the chemical form of Se [52]. Thus, in recent years the development of new NSAID analogs based on the combination of NSAID and Se entities through different Se functionalities have attracted great attention (Fig. 1). In this context, a glutathione conjugate of celecoxib (selenocoxib-1-GSH, Fig. 1) showed potent tumor growth inhibition associated with the suppression of COX-2 and PI3K/AKT signaling pathways [56]. The development of Se-NSAID analogs bearing selenocyanates and trifluoromethyl selenides attached through an amide group has also been studied. Interestingly, Se-aspirin (Fig. 1) analog was found to be > 10 times more potent than 5-FU in colorectal cells [57]. Other Se-aspirin derivatives with a longer elongation of the chain (Fig. 1) were also explored, displaying potent cytotoxic activity and inducing apoptosis in breast cancer cells [58]. Se-Flurbiprofen (Fig. 1) was an ester-linked Se-NSAID analog later reported that showed great cytotoxic activity and down-regulated the expression of Bcl-2 and up-regulated IL-2 and caspase-8 activity [59]. A Se-sulindac derivative (Fig. 1) stood out among a methylseleno-NSAID series with impressive cytotoxic activity and a unique therapeutic profile [60]. Remarkably, a selenazolidine derivative of ASA, namely AS-10 (Fig. 1), was recently found to induce caspase-mediated apoptosis, and decrease the cytokine tumor necrosis factor-alpha (TNF-α)-stimulated NF-κB nuclear translocation, the DNA binding activity and the degradation of cytosolic inhibition of κB protein [61].

Furthermore, over the last decade, our research group has also reported the synthesis and biological evaluation of selenoester derivatives with anticancer effects [62–64]. Continuing with this effort, and taking into account the abovementioned chemotherapeutic activity of NSAIDs, the promising anticancer profile of Se compounds and the reported literature that corroborate the chemical modification of NSAID scaffolds to afford more potent anticancer drugs, we report in the present work a

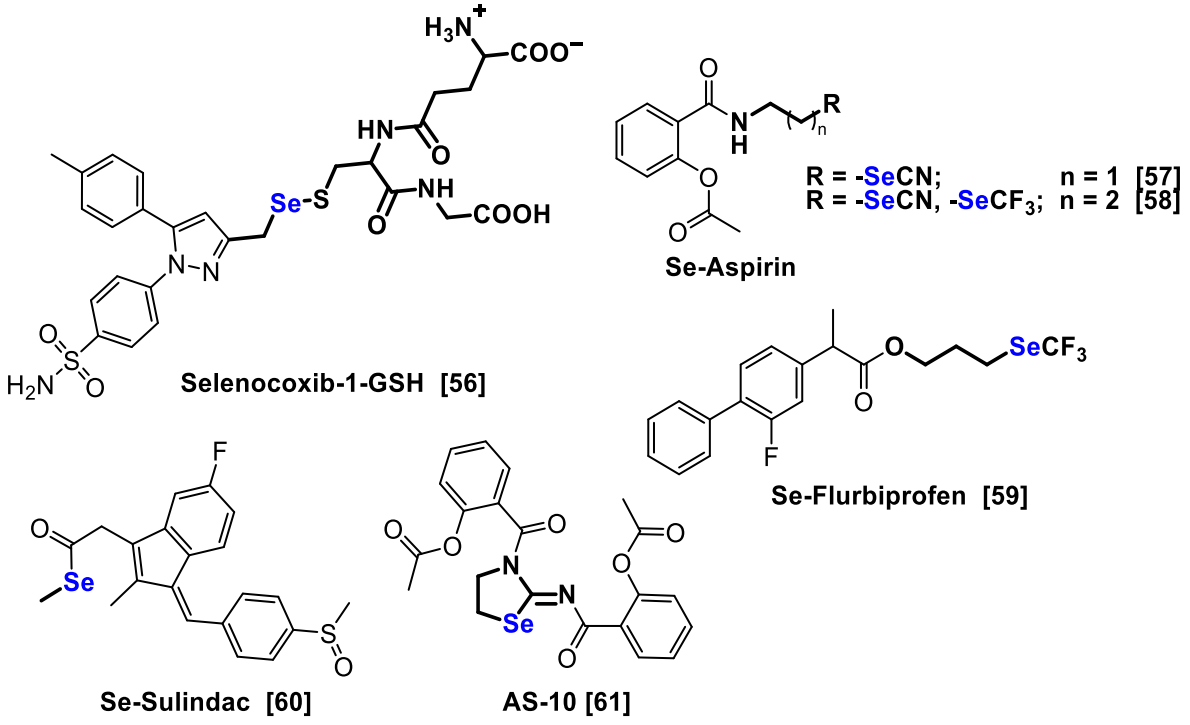

Fig. 1. Chemical structures of some NSAID derivatives containing Se.

novel series of selenoester-NSAID hybrid analogs. The rationale of this design resides in the possible hydrolysis of the selenoester group modulated with the incorporation of different functional groups attached to the Se atom of the selenoester, thus releasing active fragments.

We describe the synthesis of twenty-five new Se-NSAID compounds, along with the evaluation of their cytotoxic activity in a panel of cancer cell lines. The selectivity of the new compounds has also been assessed. The most active and selective compounds **4a**, **4b**, **4d**, **3e** and **4e** have been evaluated against other cancer cells and submitted to the National Cancer Institute's (NCI) Developmental Therapeutics Program (DTP) for cytotoxicity screening. The anticancer effect of compounds **4a** and **4d** has been further examined in two breast cancer cell lines. Compound **4d** was also subjected to a metabolite study. To our knowledge, this is the first study that reports the effect of different substituents in selenoester-modified NSAID derivatives.

2. Results and discussion

2.1. Structural design

In recent years, NSAIDs have attracted interest for their efficacy in preventing and treating cancer at different stages of the disease progression, and their anticancer activity has been widely reported [60]. Besides, several compounds bearing Se have shown their effect as chemopreventive and chemotherapeutic agents in preclinical models [65]. Taking into account all of the abovementioned facts, we hypothesized that the combination of NSAIDs and selenoester scaffold in the same molecule could lead to novel Se-NSAID analogs with increased antitumor efficacy as compared to their parent NSAIDs. The selenoester scaffold is modulated by the inclusion of different functional groups in the moiety bound to the Se atom of the selenoester, which might be easily hydrolyzed due to its analogy with an ester bond. Thus, a total of 25 new selenocompounds were obtained comprising selenoesters decorated either with carboxylic functionalities in the form of acids, esters and amides, or with nitrile groups in hydrocarbon chains of different elongation, according to the general structure shown in Fig. 2. These functionalities have been chosen to investigate the effect of the substitution of the carboxylic groups and to explore whether the length of the aliphatic chain is an important feature for biological activity. Five NSAIDs were selected to encompass a variety of chemical structures, such as salicylates (ASA and salicylic acid, Salic) and arylpropionic (naproxen, Nap and ketoprofen, Ket) and acetic (indomethacin, Ind) acid derivatives. The anticancer activity of these NSAID scaffolds has been demonstrated in several previous studies [57–61].

2.2. Chemistry

The synthesis of the novel Se derivatives of ASA (**1**), Nap (**3**), Ind (**4**) and Ket (**5**) were carried out by first reacting the corresponding NSAID acyl chloride with an aqueous solution of sodium hydrogen selenide (NaHSe), as it has been previously reported with slight modifications [62], followed by the reaction in situ of the resulting Se-NSAID sodium salt with different alkyl bromides. Additionally, the reaction of the aspirinyl chloride (**1**) with NaHSe and the corresponding bromides also yielded the salicylic derivatives **2a-e** as byproducts due to the hydrolyzation of the acetyl group in the ASA scaffold, and so these compounds were obtained with poor yields (<15% in all cases) in comparison with the rest of the series. The synthesis strategies of these derivatives are outlined in Scheme 1. All the compounds were purified by silica gel column chromatography or flash chromatography with a gradient of hexane and ethyl acetate as eluent.

For compounds **1-5c**, the starting bromide was not commercially available and had to be synthesized. As shown in Scheme 1B, 2-bromo-N-methylacetamide was obtained by treating a solution of methylamine in methylene chloride with bromoacetyl chloride in the presence of potassium carbonate. The precipitation of white crystals was observed after removing the solvent *in vacuo*. The 2-bromo-N-methylacetamide was obtained with a 40% yield and used without further purification for the synthesis of Se-NSAID derivatives **1-5c**.

The structures of all the compounds were confirmed by high-resolution mass spectrometry (HRMS) and by ^{1}H, ^{13}C and ^{77}Se nuclear magnetic resonance (NMR), as described in the Experimental Section. Inspection of ^{1}H NMR spectra of the compounds revealed the presence of two microsatellites reflecting the coupling of ^{77}Se with ^{1}H in the signal belonging to the methylene group directly attached to the Se atom. Interestingly, in the cases of the arylpropionic acid derivatives (Nap **3** and Ket **5**) this interaction is also observed in an additional split of this signal with variable coupling constant values ($J_{Se\text{-}H}$ = 2.5–12 Hz) as a consequence of this coupling between atoms. Regarding ^{13}C NMR, the peak most shifted downfield corresponds to the signal belonging to the carbonyl group of the selenoester bond (Se–C═O) in all the compounds regardless of the presence of other carbonyl groups in their structures, with an overall chemical shift between 187.5 and 203.3 ppm. Carbonyl of the ASA analogs **1a-e** appeared at the lowest range 187.5–192.9 ppm, whereas the same peak in the structural analogs of Salic derivatives **2a-e** showed signals in the range of the rest of the Se-NSAID compounds, with an interval of 192.9–198.9 ppm. Se-NSAID compounds modulated with a carboxylic derivative in the form of acids, esters or amides also showed characteristic peaks of each series. The peak belonging to the carbonyl of the acid derivatives **1-5a** appeared at ~175 ppm, whereas the corresponding peak of the carbonyl in the cases of the ester (**1-5b**) or amide (**1-5c**) series was shifted upfield to ~170 ppm as a consequence of the

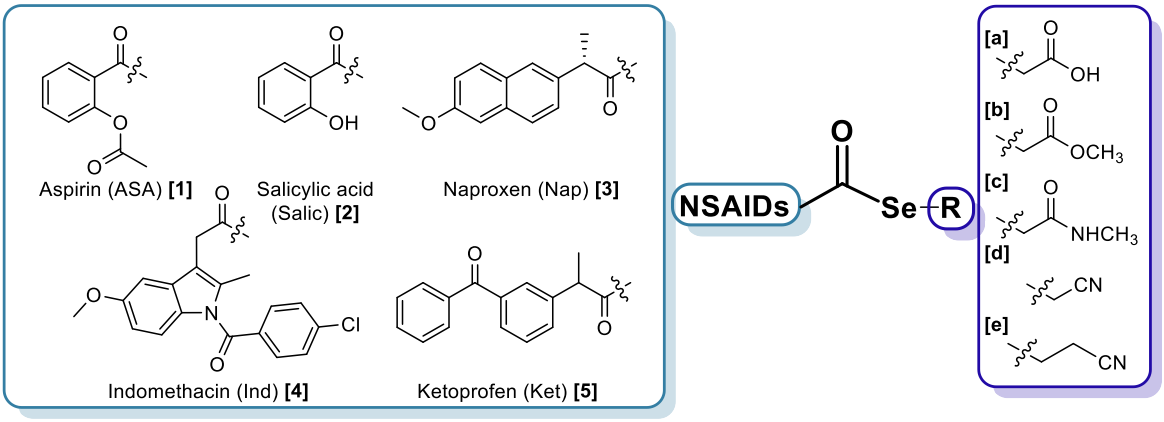

Fig. 2. General structure of the new Se-NSAID derivatives.

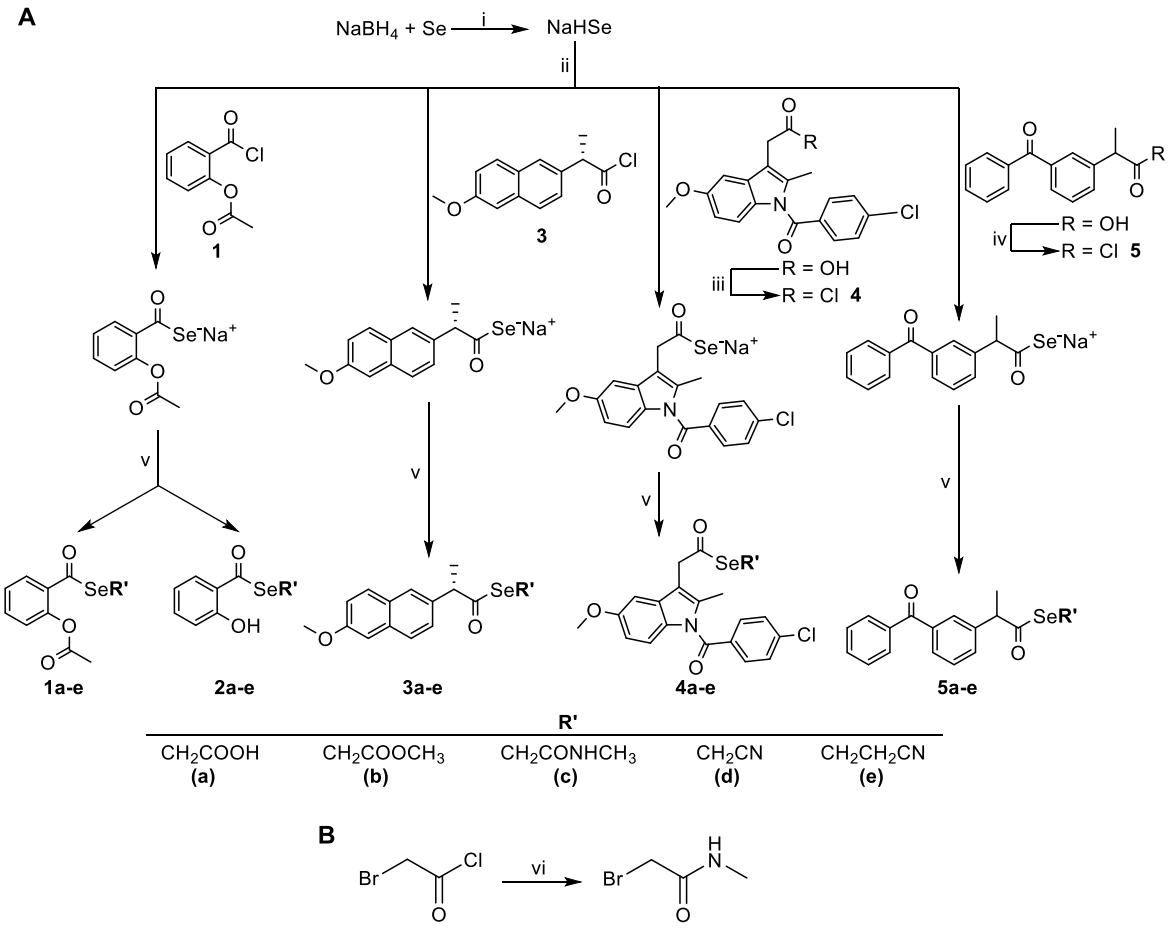

Scheme 1. Syntheses of the Se-NSAID compounds and the 2-bromo-N-methylacetamide for **1-5c** derivatives. Reagents and conditions: (i) H_2O, room temperature; (ii) THF/H_2O, 15 min, room temperature; (iii) ClCOCOCl, CH_2Cl_2, 12 h, room temperature; (iv) ClCOCOCl, CH_2Cl_2/*N*,*N*-DMF, 12 h, room temperature; (v) $BrCH_2COOH$, $BrCH_2COOCH_3$, $BrCH_2CONHCH_3$, $BrCH_2CN$ or $BrCH_2CH_2CN$, THF/H_2O, 1 h, room temperature; (vi) NH_2CH_3, K_2CO_3, CH_2Cl_2, room temperature, 4 h.

substituents of the carboxylic group. Minimal differences can also be found in the nitrile (CN) groups of series **1-5d** and **1-5e**. When the nitrile group is linked to the Se atom through a single methylene group (**1-5d**), the corresponding signal appeared at ~117 ppm, but this same group attached with a longer elongation of the chain (**1-5e**) appeared slightly shifted downfield at ~119 ppm. Concerning ^{77}Se NMR, overall the Se signal for the selenoesters appeared as one sharp peak in the range of 536–636 ppm. Among them, the signal of the **1-5d** series with only a methylene group between the nitrile and the Se atom was the most downfield shifted, appearing in the range of 582–636 ppm. Compounds of series **1-5b** and **1-5e** showed the same chemical shift for the Se peak despite the different substituents of the selenoester group, the NSAID involved being the only cause for the displacement of the signals. Likewise, when comparing the chemical shifts of the Se peak among the different NSAIDs within the same series, ASA (**1a-e**) and Ind (**4a-e**) derivatives tended to have the Se signal shifted downfield (581–636 ppm) with practically no differences between them with respect to the other NSAID derivatives. Interestingly, the salicylic acid analogs **2a-e** showed the opposite behavior, by showing the lowest range among the series with Se peaks in the interval of 536–582 ppm. ^{77}Se spectra of the arylpropionic acid derivatives of Nap (**3a-e**) and Ket (**5a-e**) revealed average chemical shifts of the Se signal (561–612 ppm), with no significant differences between them just as in the case of the Se-NSAID compounds of ASA (**1a-e**) and Ind (**4a-e**), probably due to the similar chemical environment for the Se atom in both the NSAIDs.

2.3. Evaluation of the antiproliferative activities of the novel Se-NSAID derivatives

To determine the effect of the new Se-NSAID compounds on cell viability, we first screened the 25 derivatives against a panel of four different cancer cell lines: HTB-54 (human lung carcinoma), DU-145 (human prostate carcinoma), HT-29 (human colon carcinoma) and MCF-7 (human breast carcinoma) using the 3-(4,5-dimethylthiazol-2-yl)-2,5-diphenyltetrazolium bromide (MTT) assay as previously described [66]. These four cell lines were treated for 48 h with each compound at two concentrations (10 and 50 μM). As shown in Fig. S1A, the Se-NSAID derivatives containing a nitrile moiety with either one (**1-5d**) or two (**1-5e**) methylene groups displayed a potent cell growth inhibition and even cell death at 10 μM in every cancer cell line tested. Compounds with an ester group attached to the selenoester (series **b**) exhibited the highest activity among the carboxylic derivatives, with a cell growth below 20% in the four lines tested. On the contrary, the substitution with a methylamide group (**1-5c**) led to a significant loss in the antiproliferative activity when compared to the other series derived from carboxylic moieties (**1-5a** and **1-5b**). The presence of the acid group also led to less active compounds, since only compound **4a** derived from Ind showed cell growth below 50% in at least three of the cell lines tested. Interestingly, as reported in Fig. S1B, at 50 μM concentration, almost all the compounds led to cell death. The compounds that showed cell growth inhibition above 60% in the cell lines tested at the lowest concentration were selected to further investigate the cytotoxicity at seven concentrations between 0.5 and 100 μM. Thus, all the

compounds from series **d** and **e**, along with Ind derivative from a carboxylic acid **4a** and the compounds from series **b** with a methylester moiety were evaluated in the four cell lines described before. The rest of the compounds from series **a** were also examined in the two cell lines for which they showed better activity. The corresponding parent NSAIDs (ASA, Salic, Nap, Ind and Ket) were tested as well for comparison. Since the lack of selectivity toward cancer cells is associated with unwanted side effects, the Se-NSAID derivatives were also evaluated in mammary gland (184B5) and bronchial epithelium (BEAS-2B) nonmalignant cell lines and the selectivity indexes (SI) were determined as the ratio of the IC_{50} values obtained for the nonmalignant cells and the homolog cancer cells. The calculated IC_{50} and SI values for these compounds are shown in Table 1. The GI_{50}, TGI and LD_{50} values were also determined and are included in Table S1.

The selected cancer cell lines displayed different sensitivity profiles, the breast cancer cells MCF-7 being less sensitive to the compounds than the rest of the cancer cell lines, as presented in Table 1. In this context, only compound **4a** showed an IC_{50} value in the low micromolar range. On the contrary, Se-NSAID derivatives exhibited moderate to high antiproliferative activities in general with IC_{50} values in the low micromolar range in lung (HTB-54), prostate (DU-145) and colon (HT-29) cancer cells. As presented in Table 1, the introduction of the selenoester moiety in the structure of NSAIDs led to far more potent analogs when compared to the parent drug. However, the enhancement observed is not only the result of incorporating Se in this chemical form into the NSAID, but a combination of the presence of different moieties attached to the selenoester group is also determinant for the antiproliferative activity. In this context, compounds **1-5d** and **1-5e** showed the highest activity with outstanding IC_{50} values in the low micromolar range below 10 μM in three of the four cancer cell lines, indicating that the inclusion of the nitrile group might be optimal for the antiproliferative activity. The combination of selenoester with methylester in derivatives **1-5b** also led to a more potent activity profile when compared to acid derivatives (**1-5a**).

As reported in Table 1, several compounds with potent antiproliferative activity also showed poor selectivity, with cytotoxicity towards nonmalignant cells (184B5 and BEAS-2B). However, Ind derivatives **4a** and **4d** displayed fair SI values higher than 5-fold in breast cells. Interestingly, another Ind derivative **4b**, was the most selective compound of series **b**. As for the lung cells, compounds **3e** and **4e** were also slightly more selective towards cancer cells than their counterparts. Besides, these five compounds inhibited cell growth without leading to cell death in breast nonmalignant cells (Table S1). Taken all these results together, four Ind derivatives (**4a**, **4b**, **4d** and **4e**) and one Nap derivative (**3e**) were selected as the lead compounds of each series for further studying their cytotoxicity in other breast and lung cancer cell lines. The cytotoxicity of the five compounds was therefore evaluated in two breast cancer cells (T-47D and MDA-MB-231) and/or two lung cancer cells (H1299 and A549) depending on the selectivity by which they were chosen. These results are expressed as IC_{50} values and are summarized in Table 2 collectively with the results already shown for HTB-54, MCF-7, 184B5 and BEAS-2B cells for clarity. GI_{50}, TGI and LD_{50} values were also calculated and are included in Table S2. Dose-response curves obtained for the five compounds in all the cancer cell lines tested are shown in Fig. 3.

Overall, the selected compounds showed consistency with the previous results displayed for these cancer cells. Interestingly, compound **4d** showed great activity with an IC_{50} value below 10 μM in triple-negative breast cells (MDA-MB-231) while being non-toxic to nonmalignant cells (184B5). Two compounds of the series formed with the nitrile group attached to the selenoester through a longer hydrocarbon chain (series **e**) had been chosen for their high activity and moderate selectivity, this being the only series with more than one lead compound, and so both showed potent activity in H1299 cells. Interestingly, compound **3e** showed no activity in the other lung cell line tested (A549), suggesting a selectivity for certain cancer cells.

An overview analysis of the IC_{50} values summarized in Tables 1 and 2 revealed some structure-activity relationships that can be implied: (1) the Se atom incorporated in the form of selenoester into NSAID derivatives is a valid approach to obtain potent cytotoxic compounds; (2) the presence of an amide moiety in the carboxylic-derived selenoesters resulted in inactive compounds; (3) the introduction of a nitrile group led to the most active derivatives but with scarce selectivity regardless the elongation of the hydrocarbon chain, **4d** being the only exception as

Table 1
IC_{50} values (in μM) for the Se-NSAID analogs and the parent NSAIDs in HTB-54, DU-145, HT-29, MCF-7, 184B5 and BEAS-2B cell lines, and selectivity indexes.

Compounds	Cell line							
	HTB-54	DU-145	HT-29	MCF-7	184B5	SI[a]	BEAS-2B	SI[b]
1a	48.3 ± 0.5	n.d.[c]	n.d.	>100	>100	>1.0	10.5 ± 0.1	0.2
2a	49.9 ± 6.9	n.d.	n.d.	>100	>100	>1.0	14.4 ± 4.8	0.3
3a	49.6 ± 9.8	n.d.	n.d.	>100	>100	>1.0	16.7 ± 10.1	0.3
4a	12.0 ± 4.7	25.7 ± 5.3	12.6 ± 4.1	10.7 ± 2.1	>100	>9.3	12.9 ± 6.3	1.1
5a	54.8 ± 5.9	n.d.	n.d.	>100	34.8 ± 16.3	>0.3	49.3 ± 0.3	0.9
1b	12.5 ± 2.9	11.3 ± 2.4	11.6 ± 2.5	24.2 ± 7.5	10.0 ± 0.1	0.4	7.5 ± 0.3	0.6
2b	15.2 ± 3.0	11.9 ± 2.6	13.1 ± 3.2	31.1 ± 4.0	9.2 ± 0.4	0.3	6.4 ± 0.3	0.4
3b	20.2 ± 5.8	15.5 ± 5.8	15.6 ± 6.1	65.6 ± 13.5	22.0 ± 7.4	0.3	9.7 ± 0.1	0.5
4b	15.1 ± 2.6	9.4 ± 0.9	11.8 ± 3.9	29.8 ± 13.7	50.5 ± 2.9	1.7	9.7 ± 0.3	0.6
5b	29.8 ± 5.8	10.4 ± 1.4	10.5 ± 1.5	37.5 ± 11.8	7.7 ± 1.8	0.2	9.2 ± 0.6	0.3
1d	8.1 ± 1.7	7.5 ± 1.6	7.5 ± 1.6	15.9 ± 6.7	6.2 ± 0.4	0.4	4.9 ± 0.0	0.6
2d	8.6 ± 1.4	4.9 ± 1.5	4.9 ± 1.6	22.5 ± 4.1	7.8 ± 0.5	0.3	5.1 ± 0.0	0.6
3d	8.5 ± 1.3	7.3 ± 1.8	7.0 ± 1.6	21.2 ± 3.3	11.6 ± 2.1	0.5	6.3 ± 0.2	0.7
4d	9.5 ± 0.8	8.1 ± 1.6	8.0 ± 1.6	18.8 ± 7.1	>100	>5.3	7.0 ± 1.0	0.7
5d	9.5 ± 0.1	7.2 ± 1.4	7.2 ± 1.7	21.0 ± 7.8	12.5 ± 2.1	0.6	6.6 ± 0.2	0.7
1e	7.8 ± 1.7	6.3 ± 1.2	7.4 ± 1.2	34.7 ± 12.5	4.9 ± 1.6	0.1	5.0 ± 0.0	0.6
2e	6.2 ± 1.7	7.1 ± 2.0	7.2 ± 2.0	62.2 ± 14.9	3.5 ± 0.6	0.1	5.1 ± 0.1	0.8
3e	4.2 ± 1.7	9.0 ± 1.1	8.7 ± 0.6	51.7 ± 9.3	9.9 ± 1.2	0.2	9.3 ± 0.1	2.2
4e	6.9 ± 3.2	7.7 ± 0.5	7.6 ± 0.5	30.4 ± 7.7	6.0 ± 2.4	0.2	9.3 ± 0.1	1.3
5e	6.4 ± 1.2	7.8 ± 3.0	7.8 ± 3.1	65.2 ± 14.5	8.1 ± 2.0	0.1	6.5 ± 1.2	1.0
ASA	>100	>100	>100	>100	n.d.	–	n.d.	–
Salic	>100	>100	>100	>100	n.d.	–	n.d.	–
Nap	>100	>100	>100	>100	n.d.	–	n.d.	–
Ind	>100	>100	>100	>100	n.d.	–	n.d.	–
Ket	>100	>100	>100	>100	n.d.	–	n.d.	–

IC_{50} values are presented as the mean ± SD of at least three independent experiments determined by the MTT assay. [a]SI calculated in breast cells as IC_{50} (184B5)/IC_{50} (MCF-7). [b]SI calculated in lung cells as IC_{50} (BEAS-2B)/IC_{50} (HTB-54). [c]Experiment not done.

Table 2
IC_{50} values (in μM) of **4a**, **4b**, **4d**, **3e** and **4e** derivatives in breast and lung cell lines.

Comp.	Breast cell lines				Lung cell lines			
	MCF-7	T-47D	MDA-MB-231	184B5	HTB-54	H1299	A549	BEAS-2B
4a	10.7 ± 2.1	35.1 ± 6.5	31.8 ± 15.2	>100	12.0 ± 4.7	n.d.[a]	n.d.	12.9 ± 6.3
4b	29.8 ± 13.7	23.7 ± 2.8	24.3 ± 3.1	50.5 ± 2.9	15.1 ± 2.6	n.d.	n.d.	9.7 ± 0.3
4d	18.8 ± 7.1	18.2 ± 1.6	6.3 ± 1.3	>100	9.5 ± 0.8	n.d.	n.d.	7.0 ± 1.0
3e	51.7 ± 9.3	16.8 ± 3.2	22.9 ± 3.1	9.9 ± 1.2	4.2 ± 1.7	4.9 ± 0.2	>100	9.3 ± 0.1
4e	30.4 ± 7.7	22.0 ± 6.0	24.7 ± 4.3	6.0 ± 2.4	6.9 ± 3.2	10.4 ± 3.5	24.2 ± 1.3	9.3 ± 0.1

[a] Experiment not done.

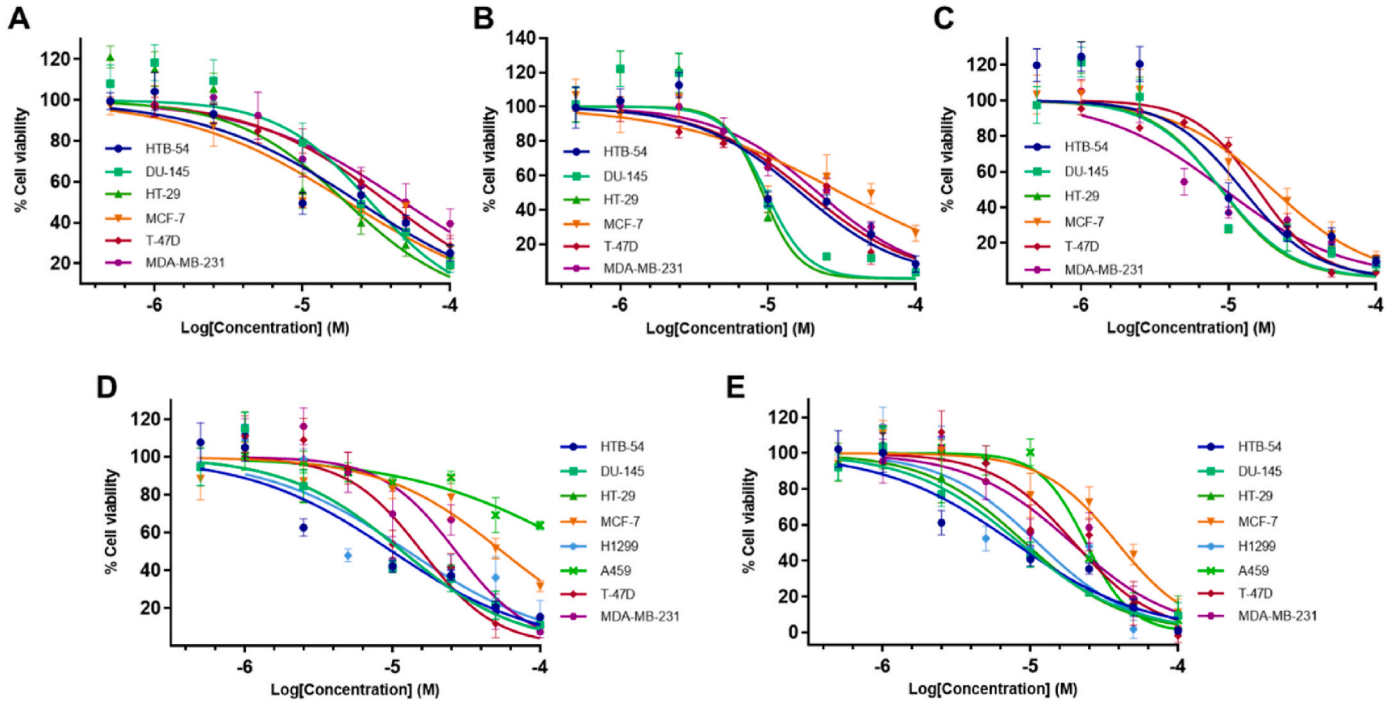

Fig. 3. Se-NSAID derivatives reduced cell viability in several cancer cell lines. Cancer cell lines were treated with seven increasing concentrations of the compounds for 48 h and the cell viability was measured by the MTT assay. (**A**) Dose-response curves of compound **4a**. (**B**) Dose-response curves of compound **4b**. (**C**) Dose-response curves of compound **4d**. (**D**) Dose-response curves of compound **3e**. (**E**) Dose-response curves of compound **4e**. Calculated IC_{50} values are shown in Tables 1 and 2 GI_{50}, TGI and LD_{50} values are included in Tables S1 and **S2**.

it stood out with a good selectivity towards breast cancer cells while evincing potent cytotoxicity; (4) NSAID Ind yielded the best NSAID derivatives in terms of activity and selectivity, as four of the five selected lead compounds were based on an Ind core.

2.4. NCI-60 analysis of the selected compounds

To further explore the cytotoxicity of these compounds, Se-NSAID derivatives **4a**, **4b**, **4d**, **3e** and **4e** were submitted to the NCI's DTP for testing in a panel of 60 human cancer cell lines [67]. Thus, **4a** [NSC: 829493], **4b** [NSC: 829494], **4d** [NSC: 829495], **3e** [NSC: 832803] and **4e** [NSC: 829496] were screened at one dose (10 μM) for 48 h of treatment. The results of this initial screening are displayed in Figs. S2–S6. Compound **4a** showed highly selective cytostatic activity in non-small cell lung and central nervous system (CNS) cancer cells, with a growth percent (GP) lower than 6% and 12% in NCI–H460 cells and SF-295, respectively. Interestingly, among all the breast cancer cells tested, this compound proved to be more active in the MCF-7 cell line (Fig. S2), in concordance with our in-house results. As shown in Fig. S3, compound **4b** demonstrated potent and selective cytotoxic activity in leukemia (HL-60(TB) cell line, GP value of-20.85%), melanoma (LOX IMVI cell line, GP value of −54.94%) and breast cancer (MDA-MB-468, GP value of −18.36%); these 3 cell lines being the only ones among their respective types that were highly sensitive to this derivative. Compound **4b** was also selectively cytostatic in CNS (SF-295), ovarian (NCI/ADR-RES) and renal (UO-31) cancers, with GP values around 9%. Compound **4d** showed potent anticancer activity in most NCI-60 cell lines, displaying overall a GP mean value of 8.01% (Fig. S4). The cytotoxic activity of this compound was remarkably potent and selective towards only a cell line in leukemia (HL-60(TB) cell line, GP value of −14.03%), melanoma (LOX IMVI cell line, GP value of −35.77%), non-small cell lung (NCI–H522 cell line, GP value of −51.25%), colon (HCT-116 cell line, GP value of −46.72%) and breast cancers (MDA-MB-468 cell line, GP value of −43.15%). Interestingly, compounds **4b** and **4d** displayed a similar biological profile with selectivity towards the same cell lines tested within the same cancer type, although **4d** showed higher cytotoxicity overall. On the contrary, compound **3e** proved to be the most cytotoxic of all the compounds submitted, with a GP mean value of −47.69% (Fig. S5). Surprisingly, **3e** was also selective towards the same leukemia cells as the previous compounds (HL-60(TB) cell line, GP value of −42.46%) but displayed poor selectivity in the rest of the cancer types. In this context, **3e** was highly active in all the non-small cell lung (with GP values between −95.58 and −21.58%) and CNS cancers (GP values between −95.33 and −45.81%), as well as in all the melanoma cell lines (GP values between −76.89 and −37.92%). Besides, compound **3e** was also found to be cytotoxic in almost every cell

line of ovarian (GP values < −40% in some cell lines) and renal cancers (GP values below −50% in seven out of eight cell lines tested), and induced cell death particularly in MDA-MB-231 (GP value of −59.86%) and MDA-MB-468 (GP value of −56.61%) breast cancer cells. As shown in Fig. S6, compound **4e** was also highly effective against several cell lines, with a GP mean value of −14.56% overall. Analog **4e** was remarkably potent in leukemia (HL-60(HB) cell line, GP value of −43.78%), melanoma (SK-MEL-5 cell line, GP value of −73.44%), colon (HCT-15 and HT29 cell lines, GP values of −64.70 and −31.21%, respectively), ovarian (IGROV1 and OVCAR-3 cell lines, GP values of −55.56 and −30.69%, respectively) renal (SN12C and TK-10 cell lines, GP values of −82.55 and −74.74%, respectively) and breast cancers (BT-549 and MDA-MB-468 cell lines, GP value of −59.78 and −35.98%, respectively). Interestingly, this compound was cytotoxic in almost every CNS cancer cell line tested (with GP values between −82.91 and −30.01%), and even in the only cell line in which this compound was not so active (U251), the GP value was still very low (1.11%). Compound **4e** also displayed potent activity in non-small cell lung cancer, with GP values in the range of −82.46% to −48.14% in four of the cell lines tested. Since the only difference in the structure of compounds **4d** and **4e** is the elongation of the hydrocarbon chain attached to the selenoester and linked to the nitrile group, it could be hypothesized that a longer chain could lead to a compound with more potent cytotoxic activity, but with less selectivity towards cancer cell lines.

Taking into account the selectivity and anticancer activity displayed by the lead compounds both in the NCI's panel of 60 cell lines and in our experiments, Se-NSAID derivatives **4a** and **4d** were selected for further biological studies due to their activity in breast cancer cells, with IC_{50} values of 10.7 μM in MCF-7 cells and 6.3 μM in MDA-MB-231 cells respectively (Table 2). Furthermore, **4a** and **4d** also showed the best selectivity among all the compounds tested in breast cells (Table 1).

2.5. Solubility and stability studies of selected Se-NSAID derivatives

A preliminary study of the physico-chemical properties of **4a**, **4b**, **4d**, **3e**, and **4e** was also performed. Since the solubility in aqueous medium is a key factor in the pharmacological performance and bioavailability of a compound, this feature was determined for selected selenoderivatives based on their biological activity. Thus, the corresponding water solubility parameter ($logS_m$) was obtained by both *in silico* and *in vitro* methods and is shown in Table 3 for compounds **4a** and **4d**. The solubility of compounds **4b**, **3e** and **4e** was also calculated and included in the Supplementary data (Table S4). Likewise, the acid dissociation constant (pK_a) and the lipid/water partition coefficient (ClogP) values were calculated with the ChemDraw software and are also included in Table 3 and S4.

Overall, all the Se-NSAID derivatives showed moderately low solubility, as in the case of other selenocompounds reported in the literature [68]. In general, the same tendency could be observed for the $logS_m$ values calculated with the computational programs SwissADME and OSIRIS. Hence, the solubility calculated *in silico* predicted that the Nap-derived compound **3e** would display the highest solubility among the Se-NSAID derivatives (Table S4). However, the experimental solubility values revealed that the Ind-derived **4a** with a carboxylic acid was the most soluble compound, followed by derivative **4d** (Table 3). Notably, the presence of an additional nitrile group in the aliphatic chain attached to the selenoester group yielded compounds with the lowest $logS_m$ values (**3e** and **4e**) experimentally. The low solubility showed by compound **4e** in the experimental method was in concordance with the predicted value *in silico* (Table S4). The lipophilic behavior of the Se-NSAID derivatives was also confirmed by the ClogP obtained (Table 3 and **S4**). Likewise, although all the values determined were lower than 5, compound **3e** showed the lowest ClogP value (3.42, Table S4), as in the case of the $logS_m$ also calculated *in silico*. Due to the presence of a carboxylic acid group, **4a** was the only derivative among the selected compounds which presented a pK_a value (Table 3).

Table 3
Aqueous solubility, ClogP and pK_a values of selected Se-NSAID derivatives determined with computational and experimental methods.

Compound	Experimental aqueous solubillity		Aqueous solubility calculated *in silico*		ClogP (ChemDraw)	pK_a (ChemDraw)
	[g/L]	$logS_m$[a]	$logS_m$ (SwissADME)	$logS_m$ (OSIRIS)		
4a	0.011	−4.65	−5.10	−4.85	4.64	4.22
4d	0.009	−4.70	−5.18	−5.52	4.38	N/A[b]

[a] $logS_m$: calculated based on solubility S_m (mol/L).
[b] N/A: not applicable.

The fact that the Se-NSAID derivatives could undergo hydrolysis was considered in the design of the new selenocompounds. Thus, the possible hydrolysis of derivatives **4a** and **4d** were further explored, as shown in Fig. 4. Although both derivatives showed a similar profile at short times, the exposure to a 10% of D_2O for longer times revealed that compound **4a** was hydrolyzed to a greater extent than compound **4d**. Nevertheless, at the end of the experiment derivatives **4a** and **4d** presented a 60% and 50% of hydrolysis, respectively.

Furthermore, the stability of compounds **4a** and **4d** was also assessed in simulated gastric fluid (SGF) and simulated intestinal fluid (SIF). The results are outlined in Table 4 expressed as the relative difference (RD) calculated by high-performance liquid chromatography (HPLC).

Remarkably, both compounds underwent a significant hydrolysis under these conditions, confirming that they could be susceptible of being modified by proteolytic enzymes. This effect was more pronounced in SGF at pH 1.2 for compound **4a**, which could be additionally affected by the acidic medium due to the presence of its carboxylic acid group. On the contrary, compound **4d** was more stable in SGF (Table 4), although an immediate hydrolysis was observed for this derivative in SIF at pH 6.8. Importantly, a RD value higher than 5% denotes a significant degradation and potential instability in the gastrointestinal tract [69], thus suggesting that these compounds would not be suitable for oral administration.

2.6. Compounds *4a* and *4d* inhibited the cell viability of breast cancer cells

To further support the antiproliferative results obtained with the MTT assay (Table 1–**2** and Fig. 3), we performed the trypan blue dye exclusion assay [70] in MCF-7 and MDA-MB-231 cells with compounds

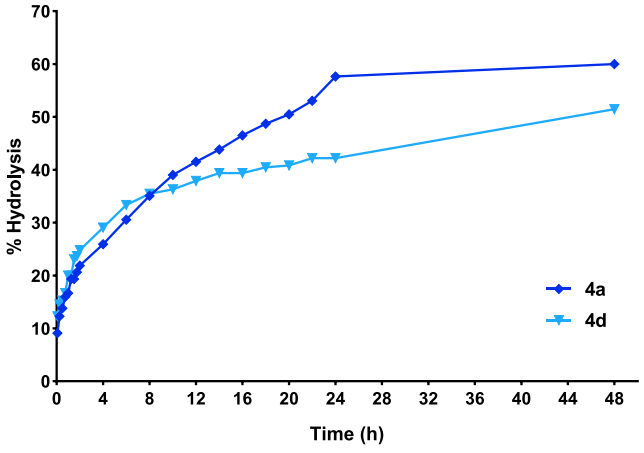

Fig. 4. Hydrolysis study of compounds **4a** and **4d** calculated by q-^{1}H NMR spectra analysis of each compound dissolved in a DMSO-d_6 solution containing 10% D_2O for 48 h.

Table 4
Stability of lead compounds **4a** and **4d** in SGF (pH 1.2, pepsin 3.2 mg/mL) and in SIF (pH 6.8, pancreatin 10 mg/mL) expressed as the percentage of RD values.

Time point (min)	4a		4d	
	SGF	SIF	SGF	SIF
0	Immediate	–	–	Immediate
5	hydrolysis	68.18 ± 6.88	1.72 ± 2.24	hydrolysis
15		73.21 ± 0.42	3.63 ± 1.17	
30		59.36 ± 1.16	43.39 ± 14.46	
60		61.59 ± 2.74	33.31 ± 1.46	
120		63.73 ± 0.19	33.08 ± 0.15	
240	n.d.[a]	67.56 ± 6.87	n.d.	

RD values are presented as the mean ± SD of two independent experiments. [a]Experiment not done.

4a and **4d**. Cells were treated with three concentrations of each compound (5, 10 and 25 μM) and the population of alive cells after treatment was calculated at two different time points (24 and 48 h). As shown in Fig. 5, the inhibition of cell viability was time- and dose-dependent for both the compounds in the two cell lines tested. In MCF-7 cells, at 24 h (Fig. 5A) compound **4a** showed no difference with respect to the cells treated with vehicle (DMSO) at 5 μM, but a higher concentration of compound reduced the viability of the cells significantly. This difference was evinced at 48 h too (Fig. 5B). Interestingly, at 10 and 25 μM there were less than 50% of alive cells at 48 h treatment with this compound, even in MDA-MB-231 cells (Fig. 5B,**D**). Nevertheless, compound **4d** was significantly more cytotoxic than **4a** in both the cell lines at the same concentrations even at 24 h, this effect being not significant only at lower concentrations (5 and 10 μM) in the shortest period of time (Fig. 5A,**C**). Furthermore, these differences in the activity increased with a longer treatment duration (Fig. 5B,**D**). Compound **4d** was found to be cytotoxic even at the lowest concentration tested (5 μM) in both the cell lines at 48 h, and at 25 μM there were almost no alive cells in both the cell lines at this time point (Fig. 5B,**D**). In addition, a high concentration (25 μM) of this compound proved to be cytotoxic even at 24 h with less than 40% of remaining alive cells in both cell lines (Fig. 5A,**C**). In concordance with our previous results obtained with the MTT assay, MDA-MB-231 cells were also more sensitive to compound **4d** after 48 h of treatment, the population of alive cells being highly compromised at the three concentrations tested (Fig. 5D).

2.7. Compounds *4a* and *4d* induced apoptosis in breast cancer cells

The cell viability assays performed evinced that compounds **4a** and **4d** displayed antiproliferative activity. To further confirm if these compounds could induce cell death through apoptosis, we performed the Annexin V & Dead Cell assay. Annexin V is routinely used to detect apoptosis due to its affinity for phosphatidylserine (PS) residues exposed in the surface of the cells during early apoptosis [71]. In addition, 7-AAD is used to exclude late apoptotic and dead cells, because only those cells which have their membrane permeability compromised could be stained by this marker [72]. Furthermore, it is well-known that sequential activation of caspases is essential for triggering apoptosis [73]. Executioner caspases such as caspase-3 and caspase-7 cleave many different structural and regulatory proteins that shut down the functions of the cell and thus become hallmarks of apoptosis [74]. Therefore, to confirm the results obtained with the Annexin V & Dead Cell assay, the activation of executioner caspases-3 and -7 was also studied using the Caspase 3/7 assay. Herein, a reagent with a DNA binding dye linked to a peptide substrate DEVD is released after caspase cleavage in apoptotic cells, thus staining those cells with caspase 3/7 activity. Likewise, this assay also included the dead cell marker 7-AAD.

Hence, MCF-7 and MDA-MB-231 cells were treated either with compound **4a** or **4d** for 24 h at different concentrations and results were obtained following the manufacturer's protocol. Both assays led to four different populations of cells: healthy cells (Annexin V, Caspase 3/7 and 7-AAD negative (lower left quadrant)); early apoptotic cells (both Annexin V and Caspase 3/7 positive and 7-AAD negative (lower right quadrant)); late apoptotic or dead cells (Annexin V, Caspase 3/7 and 7-AAD positive (upper right quadrant)); and necrotic cells (both Annexin V and Caspase 3/7 negative and 7-AAD positive (upper left quadrant)). Results obtained in the MCF-7 cell line are presented in Fig. 6, while the results in the MDA-MB-231 cell line are included in Fig. 7. In addition, a quantitative comparison of the difference in the cell population induced by each compound is shown in Fig. 6C,**D** and Fig. 7C,**D**. Besides, since MCF-7 cells do not express caspase-3 [75], the data assessed in this cell line is only referred as caspase-7.

In general, cells treated with vehicle (DMSO) were located mainly in the lower left quadrant, while the treatment with either compound **4a** or **4d** induced a shift from healthy cells towards an apoptotic state. This shift was almost the same for both concentrations of compound **4a** in

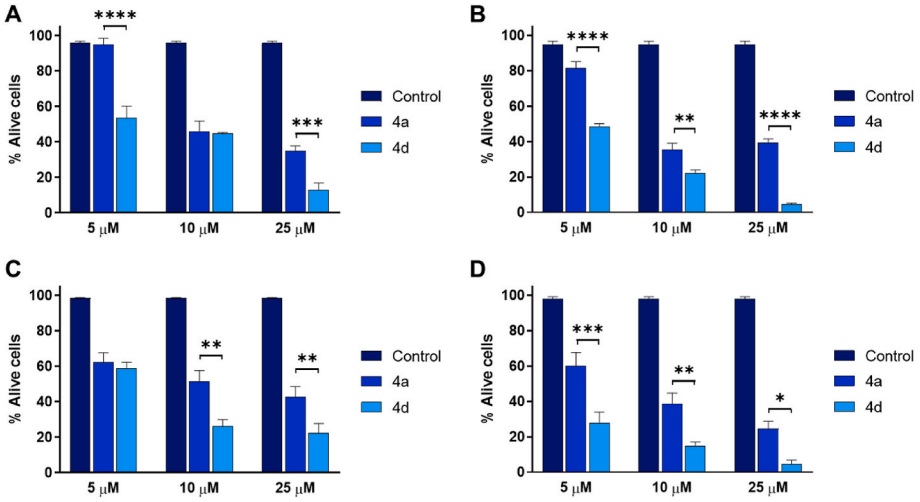

Fig. 5. Effect of compounds **4a** and **4d** on the inhibition of cell viability. (**A**) Percentage of alive MCF-7 cells after 24 h of treatment. (**B**) Percentage of alive MCF-7 cells after 48 h of treatment. (**C**) Percentage of alive MDA-MB-231 cells after 24 h of treatment. (**D**) Percentage of alive MDA-MB-231 cells after 48 h of treatment. Data are expressed as the mean ± SEM of three independent experiments. ****$p < 0.0001$, ***$p < 0.001$, **$p < 0.01$, *$p < 0.05$ when comparing compounds.

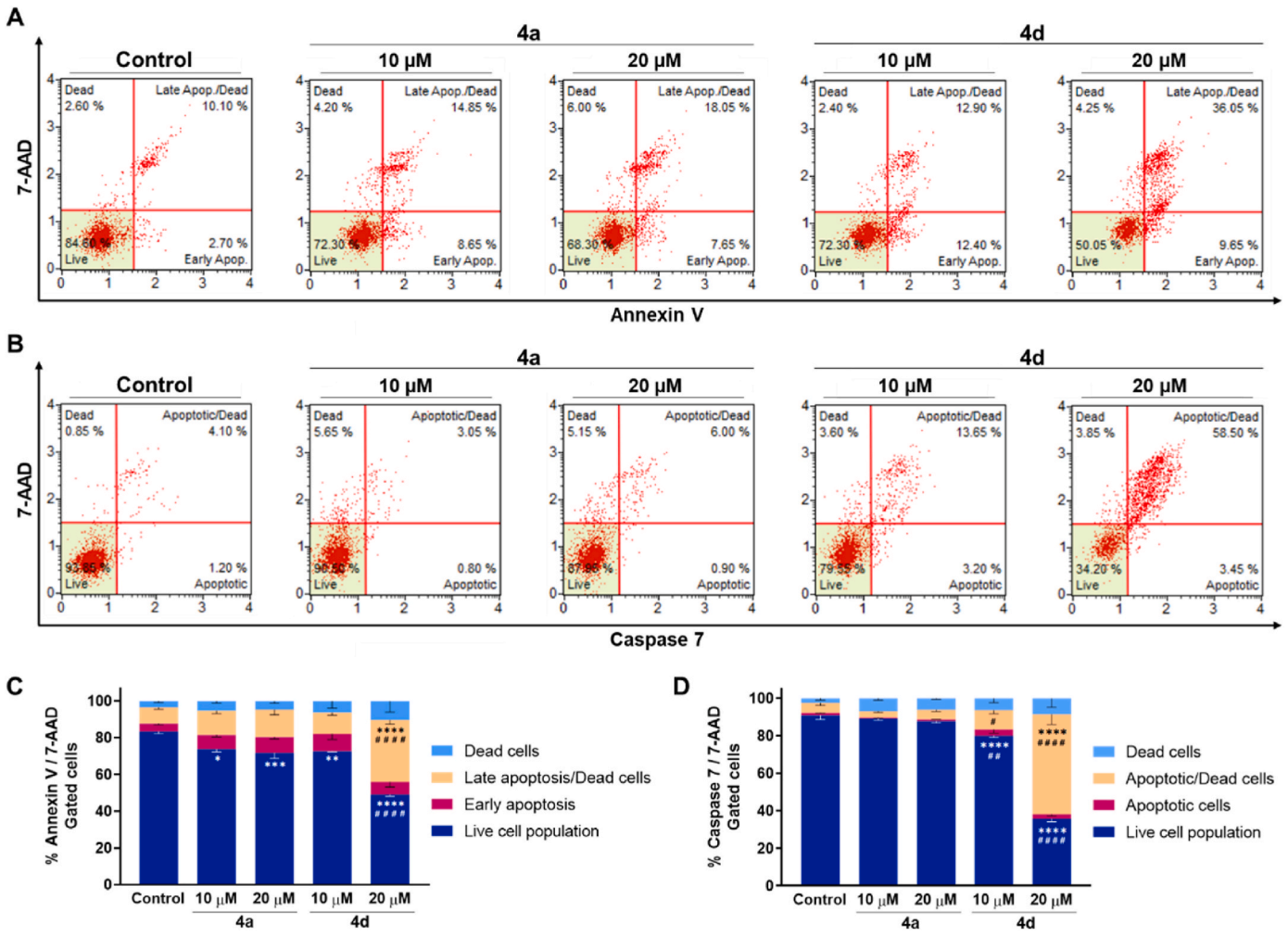

Fig. 6. Compounds **4a** and **4d** induced apoptotic cell death in MCF-7 cells. (**A**) Cells were treated with two concentrations of **4a** or **4d** for 24 h and examined on a Muse™ automated cell analyzer with the Annexin V & Dead Cell apoptosis assay. (**B**) Analogous independent experiment performed with the Caspase 3/7 apoptosis assay. (**C**,**D**) Quantification of the cell population with the Annexin V & Dead Cell and Caspase 3/7 assays, respectively. Data are presented as the mean ± SEM of three independent experiments. $^{****}p < 0.0001$, $^{***}p < 0.001$, $^{**}p < 0.01$, $^{*}p < 0.05$ when comparing control and compounds. $^{\#\#\#\#}p < 0.0001$, $^{\#\#}p < 0.01$ when comparing compounds.

MCF-7 cells in the Annexin V assay (Fig. 6A), in which the population of viable cells was decreased to ~70% while the percentage of late apoptotic or dead cells was consequently increased with respect to the control (Fig. 6A,**C**). Considering the Caspase 3/7 assay (Fig. 6B,**D**), there was a slight increase in the population of dead cells, although almost no effect was observed compared to the control at these concentrations of compound **4a**. On the contrary, compound **4d** induced apoptosis in MCF-7 cells in a dose-dependent manner (Fig. 6), in concordance with the results obtained from the cell viability assays. At 10 μM, the population of healthy cells in the Annexin V assay decreased to ~70%, this being the same effect as with compound **4a** at a double concentration, but with a slightly higher percentage of cells in an early apoptotic state (Fig. 6A,**C**). Thus, **4d** induced apoptosis more effectively than compound **4a** in MCF-7 cells, presenting a similar profile of cell population but at a lower dose (Fig. 6A,**C**). At 20 μM, the population of viable cells treated with **4d** dropped to ~50%, while more than 45% of cells were detected to be apoptotic. Besides, only a slight percentage of cells were necrotic, as there were almost no cells located in the upper left quadrant (Fig. 6A). This pattern was even more marked in the Caspase 3/7 assay (Fig. 6B,**D**), given that although at 10 μM there were more healthy cells than in the Annexin V assay at the same concentration, at 20 μM this population decreased to less than 35%, most of the cells being in an apoptotic or dead state (>60%), and only a few cells appeared in the upper left quadrant with 7-AAD positive and caspase-7 negative (Fig. 6B).

MDA-MB-231 cells were treated with a single concentration of compound **4a** or **4d** according to their values of IC_{50} (30 and 6.5 μM, respectively). As it was expected due to the previous results obtained from the MTT and the trypan blue dye exclusion assays, in MDA-MB-231 cells the compounds followed a similar pattern, compound **4d** being more active overall (Fig. 7). Similar to as observed in the case of MCF-7 cells, compound **4a** was found to induce more apoptosis in the Annexin V assay, and so the population of healthy cells was lower at the concentration used than in the Caspase 3/7 assay, although in both the experiments the cells shifted mainly to a necrotic state with either Annexin V or caspase-3/7 activity negative and 7-AAD positive (Fig. 7). This effect was higher in the Annexin V assay (Fig. 7A,**C**), with almost 22% of the cell population in the upper left quadrant and only ~5% of apoptotic cells. Interestingly, compound **4d** induced even more population of necrotic cells, with almost 30% of cells in the upper left quadrant despite being used at nearly 5-fold lower concentration than **4a**. As shown in Fig. 7B,**D**, this tendency was also maintained in the Caspase 3/7 assay, the percentage of cells with an increase in the caspase 3/7 activity being also enhanced after the treatment with compound **4d** in a more pronounced manner as compared to **4a**.

Considering all these results in both the cell lines, our data confirmed that compounds **4a** and **4d** induced apoptosis in breast cancer cells. As

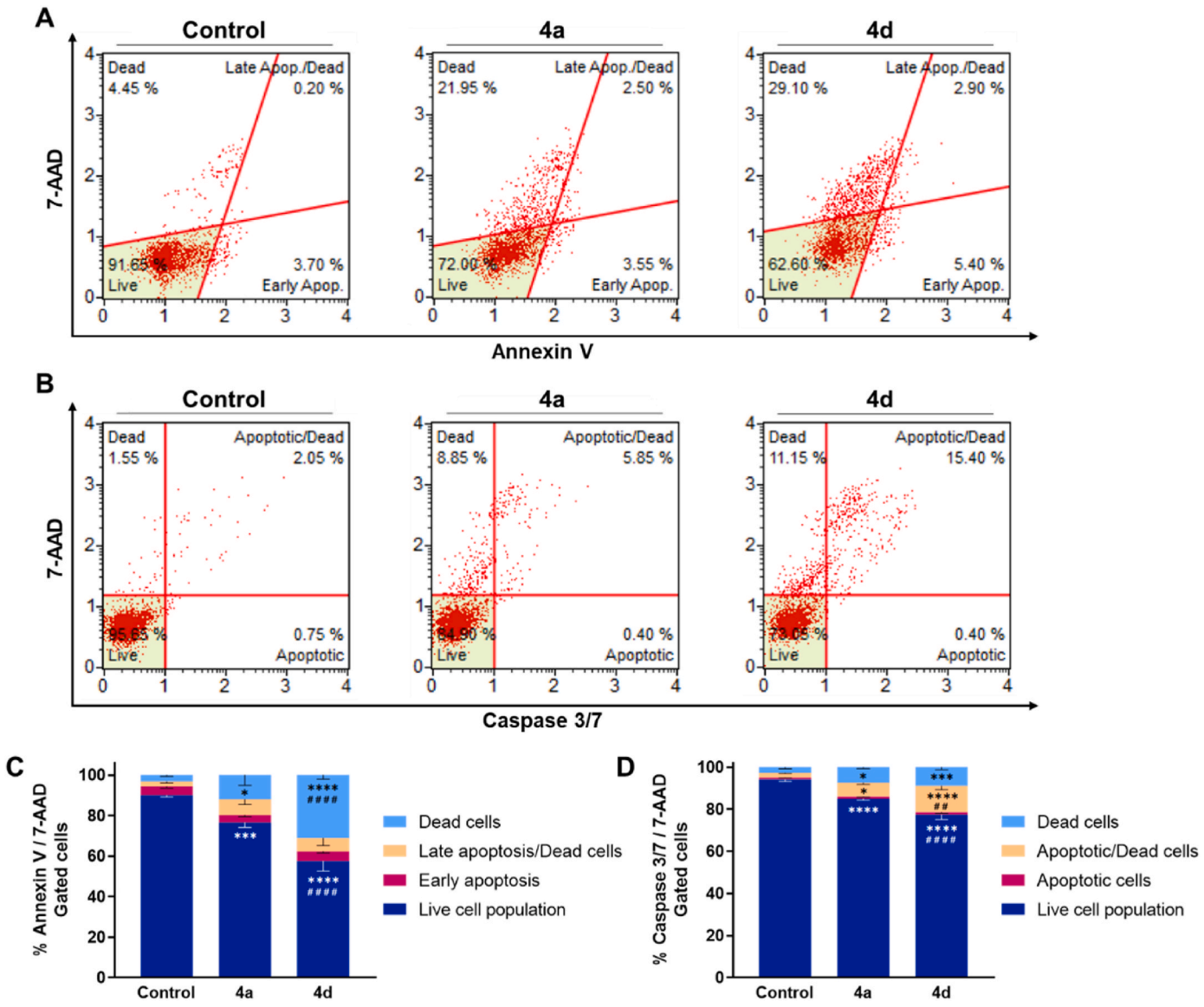

Fig. 7. Compounds **4a** and **4d** induced apoptotic cell death in MDA-MB-231 cells. (**A**) Cells were treated either with 30 μM of **4a** or 6.5 μM of **4d** for 24 h and examined on a Muse™ automated cell analyzer with the Annexin V & Dead Cell apoptosis assay. (**B**) Analogous independent experiment performed with the Caspase 3/7 apoptosis assay. (**C**,**D**) Quantification of the cell population with the Annexin V & Dead Cell and Caspase 3/7 assays, respectively. Data are presented as the mean ± SEM of three independent experiments. $^{****}p < 0.0001$, $^{***}p < 0.001$, $^{*}p < 0.05$ when comparing control and compounds. $^{\#\#\#\#}p < 0.0001$, $^{\#\#}p < 0.01$ when comparing compounds.

shown in Figs. 6 and 7, compound **4d** proved to be a potent apoptosis inducer as demonstrated by the presence of PS residues and caspase 3/7 activity enhancement, and displayed greater activity than **4a** in the two cancer cell lines tested.

2.8. *Compound **4d** was metabolized in vitro by human S9 fractions*

The prediction of the hepatic metabolism of a new therapeutic drug is essential because a biotransformation may generate active, non-active or toxic metabolites that could affect important features such as efficacy and toxicity [76]. Thus, as a first approach to evaluate the metabolic profile, lead compound **4d** was incubated *in vitro* with human S9 fractions for 60 or 120 min in a buffer solution containing NADPH, and the reaction mixtures were analyzed by HPLC with MS-TOF.

As shown in Fig. 8, metabolites derived from compound **4d** are formed after 120 min, proving the moderate stability of the lead compound. Inspection of the mass spectrometric analysis of the metabolized compound **4d** revealed that the major metabolic route could possibly be the hydrolysis of the selenoester bond, thus releasing Ind as the base peak with the highest area among all the signals (Fig. 8A). Interestingly, a metabolite bearing Se could be identified by mass spectrometry with an exact mass of 123.9671 (labeled as Metabolite 1 in Fig. 8) that could correspond to the negatively charged Se fragment separated from the Ind scaffold. As in the case of some of the other metabolites identified, the reduction of the nitrile group to a primary amine was also considered for this fragment. The rest of the metabolites determined could be related to those of typical metabolic processes of the NSAID alone (Fig. 8B). Hence, some of these metabolites contained Se, and although they were formed in lower amount than those formed by selenoester cleavage, they might also be responsible for the biological activity exhibited. These preliminary results could suggest that the rationale of our design based on the liability of the selenoester bond due to its analogy to an ester bond is a valid approach to obtain modified-Se-NSAIDs that could enable the release of the parent NSAID along with active Se species. Whether a particular metabolic pathway or all the above factors together contribute to the efficacy of compound **4d**,

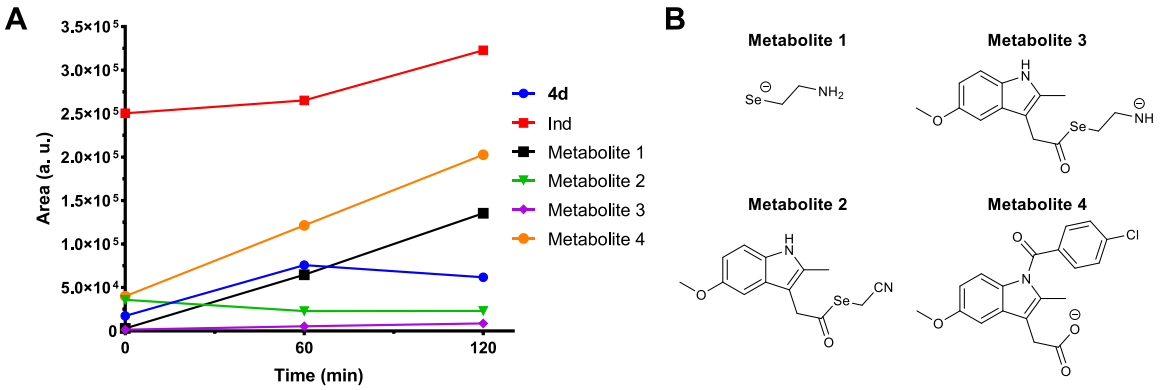

Fig. 8. The *in vitro* microsomal metabolism of compound **4d** yielded Ind and Se moiety, among other metabolites related to Ind metabolism. (**A**) The degradation of compound **4d** over 120 min was examined with human S9 fractions at two different time points after incubation in a buffer solution with NADPH. (**B**) Possible chemical structures identified by mass spectrometry.

remain to be proven in future studies.

3. Conclusions

In conclusion, the incorporation of Se into traditional NSAIDs led to potent analogs with anticancer activity. Among the 25 novel Se-NSAID derivatives synthesized in this work, compounds **4a** and **4d** stood out as the most selective compounds towards breast cancer. The selected derivatives were found to have low aqueous solubility and relatively high lipophilicity. The compounds were also susceptible of being hydrolyzed to a different extent after the exposure to aqueous and simulated gastric and intestinal media. Compounds **4a** and **4d** inhibited the proliferation of cancer cells as confirmed by the MTT and the trypan blue dye exclusion assays. Besides, compound **4d** showed low IC_{50} values and was found to be more potent than **4a** in almost every cell line tested. The better cytotoxicity profile of this compound was also supported by the results obtained in NCI's panel of 60 cancer cell lines. Furthermore, **4d** inhibited the growth of breast cancer cells by inducing apoptosis, evinced by caspase-3/7 activity and the presence of PS on the outer membrane of tumorigenic cells. Additionally, the formation of metabolites of this compound in human S9 fractions revealed the cleavage of the selenoester bond, thus releasing the parent Ind. Other possible metabolites containing Se that could contribute to the anticancer activity observed were also suggested after mass spectrometric analysis. Overall, **4d** was identified as a potential Se-containing anticancer compound with an appealing chemotherapeutic profile. The work presented here warrants future studies to further assess the *in vivo* efficacy, toxicity, and a more detailed characterization of the mechanism of action of this compound in breast cancer models.

4. Experimental section

4.1. Chemistry

Reagents, starting materials and solvents were purchased from commercial suppliers and used as received without further purification. Reaction courses were monitored by thin-layer chromatography (TLC) on precoated silica gel 60 F254 aluminum sheets (Merck, Darmstadt, Germany) and the spots were visualized under UV light. The crude reaction products were purified by silica gel column chromatography using silica gel 60 Å (0.040–0.063 mm, Merck, Darmstadt, Germany) or by flash chromatography, using hexane/ethyl acetate as the elution solvent in both cases. HRMS was performed on a Micromass Q-TOF mass spectrometer. ^{1}H-, ^{13}C and ^{77}Se-NMR spectra were recorded on a Bruker Avance Neo 400 MHz operating at 400, 100 and 76 MHz respectively, using $CDCl_3$ as solvent and TMS as the internal standard. Chemical shifts are reported in δ values (ppm) and coupling constants (J) values are reported in hertz (Hz). Melting points (mp) were determined with a Mettler FP82+FP80 apparatus (Greifensee, Switzerland). The purity of key compounds was determined by reverse phase HPLC. All compounds are >95% pure by HPLC analysis. The purity was determined by HP series 1100 HPLC, with a binary pump and a photodiode array detector (DAD), using Bondclone C18 (300 mm × 3.90 mm, 10 μm) column, mobile phase A = H_2O, mobile phase B = acetonitrile; flow rate 1 mL/min. The column was eluted with H_2O: acetonitrile (4:1) to (0:1) for 25 min. The injection volume was 10 μL (1 mg/mL acetonitrile solution) and DAD monitoring was at 258 nm.

4.1.1. Synthesis of 2-bromo-N-methylacetamide

To a mixture of methylamine (0.5 g, 1 mmol) and K_2CO_3 (2.2 g, 1 mmol) in methylene chloride (20 mL), bromoacetyl chloride (2.5 g, 1 mmol) was added. The reaction mixture was stirred at room temperature for 4 h and then filtered off. The filtrate was concentrated *in vacuo* to afford the desired product. Yield: 40%. ^{1}H NMR (400 MHz, $CDCl_3$): δ 2.87 (d, J = 4.9 Hz, 3H, NCH_3); 3.88 (s, CH_2, 2H); 6.54 (s, NH, 1H). ^{13}C NMR (100 MHz, $CDCl_3$): δ 27.1 (NCH_3), 29.3 (CH_2), 166.1 (NH–C═O).

4.1.2. General procedure for the preparation of the selenoester derivatives

NSAID acyl chloride (2 mmol) and THF (5 mL) were added to a water solution of sodium hydrogen selenide (2 mmol) formed in situ following the procedure reported by Sanmartin et al. [62]. The mixture was stirred at room temperature for 15 min and then the corresponding halide (2 mmol) was added to the reaction. After 1 h, the reaction mixture was extracted with methylene chloride (3 x 20 mL) and washed with water (2 x 30 mL). The organic layers were dried with anhydrous sodium sulfate and concentrated *in vacuo*. The crude product of the reaction was purified using silica gel chromatography or by flash chromatography with a hexane/ethyl acetate gradient. In the case of the NSAIDs Ind (**4**) and Ket (**5**), the synthesis of the corresponding acyl chloride reagent was necessary prior to the formation of the selenoester derivative. These compounds were obtained by the reaction of the carboxylic acid reagent (2 mmol) with oxalyl chloride (6 mmol) in methylene chloride (25 mL). *N*,*N*-dimethylformamide (0.1 mL) was added in the case of Ket (**5**). The mixture was stirred overnight at room temperature. The resulting product was isolated by the rotatory evaporation of the solvent and washed with methylene chloride (2 x 20 mL). The acyl chlorides were used without further purification.

2-((2-Acetoxybenzoyl)selenyl)acetic acid (**1a**). The title compound was synthesized from *O*-acetylsalicyloyl chloride, selenium, sodium borohydride and bromoacetic acid according to the general procedure described above. A pink powder was obtained. Yield: 39%; mp: 95-96 °C. ^{1}H NMR (400 MHz, $CDCl_3$): δ 2.38 (s, 3H, CH_3); 3.80 (s, 2H, CH_2);

7.18 (dd, $J = 8.1$ and 0.9 Hz, 1H, H_3); 7.36 (td, $J = 7.8$ and 1.1 Hz, 1H, H_5); 7.61 (td, $J = 7.8$ and 1.6 Hz, 1H, H_4); 7.91 (dd, $J = 7.9$ and 1.6 Hz, 1H, H_6). ^{13}C NMR (100 MHz, $CDCl_3$): δ 21.5 (CH_3), 25.6 (CH_2), 124.3, 126.6, 129.8, 130.6, 134.6, 148.0 (C_{aryl}), 169.2 (CH_3–C═O), 175.4 (OH–C═O), 189.8 (Se–C═O). ^{77}Se NMR (76 MHz, $CDCl_3$): δ 590. HRMS *m/z*: calcd for $C_{11}H_{10}O_5Se$ $[M + Na]^+$, 324.9586; found, 324.9589.

2-((2-Hydroxybenzoyl)selenyl)acetic acid (**2a**). The title compound was synthesized from *O*-acetylsalicyloyl chloride, selenium, sodium borohydride and bromoacetic acid according to the general procedure described above. A white powder was obtained. Yield: 11%; mp: 117-118 °C. ^{1}H NMR (400 MHz, $CDCl_3$): δ 3.85 (s, 2H, CH_2); 6.96 (ddd, $J =$ 8.2, 7.3 and 1.1 Hz, 1H, H_5); 7.00 (dd, $J = 8.5$ and 0.8 Hz, 1H, H_3); 7.52 (ddd, $J = 8.6$, 7.3 and 1.6 Hz, 1H, H_4); 7.72 (dd, $J = 8.1$ and 1.5 Hz, 1H, H_6); 10.34 (s, 1H, OH). ^{13}C NMR (100 MHz, $CDCl_3$): δ 24.9 (CH_2), 118.5, 120.1, 121.6, 129.9, 136.9, 158.6 (C_{aryl}), 175.0 (OH–C═O), 197.7 (Se–C═O). ^{77}Se NMR (76 MHz, $CDCl_3$): δ 542. HRMS *m/z*: calcd for $C_9H_8O_4Se$ $[M + Na]^+$, 282.9480; found, 282.9485.

*(S)-2-((2-(6-Methoxynaphthalen-*2-yl*)propanoyl)selenyl)acetic acid* (**3a**). The title compound was synthesized from (*S*)-2-(6-methoxy-2-naphthyl)propionyl chloride, selenium, sodium borohydride and bromoacetic acid according to the general procedure described above. A white powder was obtained. Yield: 9%; mp: 101-102 °C. ^{1}H NMR (400 MHz, $CDCl_3$): δ 1.64 (d, $J = 7.1$ Hz, 3H, CH_3); 3.55 (d, $J = 11.0$ Hz, 2H, CH_2); 3.93 (s, 3H, OCH_3); 4.02 (q, $J = 7.1$ Hz, 1H, CH); 7.13 (s, 1H, H_5); 7.17 (dd, $J = 8.9$ and 2.5 Hz, 1H, H_7); 7.35 (dd, $J = 8.5$ and 1.8 Hz, 1H, H_8); 7.71 (s, 1H, H_1); 7.73 (d, $J = 9.1$ Hz, 2H, H_3+H_4). ^{13}C NMR (100 MHz, $CDCl_3$): δ 17.9 (CH_3), 25.2 (CH_2), 55.5 (OCH_3), 57.4 (CH), 105.8, 119.5, 126.8, 127.7, 128.0, 128.9, 129.6, 133.2, 134.5, 158.2 (C_{aryl}), 175.4 (OH–C═O), 202.7 (Se–C═O). ^{77}Se NMR (76 MHz, $CDCl_3$): δ 572. HRMS *m/z*: calcd for $C_{16}H_{16}O_4Se$ $[M + Na]^+$, 375.0106; found, 375.0105.

*2-((2-(1-(4-Chlorobenzoyl)-5-methoxy-2-methyl-1H-indol-*3-yl*)acetyl) selenyl)acetic acid* (**4a**). The title compound was synthesized from 1-(4-chlorobenzoyl)-5-methoxy-2-methyl-3-indoleacetic acid, oxalyl chloride, selenium, sodium borohydride and bromoacetic acid according to the general procedure described above. A white powder was obtained. Yield: 38%; mp: 145-147 °C. ^{1}H NMR (400 MHz, $CDCl_3$): δ 2.41 (s, 3H, CH_3); 3.59 (s, 2H, CH_2–Se); 3.82 (s, 3H, OCH_3); 3.91 (s, 2H, CH_2); 6.70 (dd, $J = 9.0$ and 2.5 Hz, 1H, H_6); 6.87 (d, $J = 2.5$ Hz, 1H, H_4); 6.90 (d, $J =$ 9.0 Hz, 1H, H_7); 7.49 (d, $J = 8.5$ Hz, 2H, $H_{3'}$+$H_{5'}$); 7.67 (d, $J = 8.5$ Hz, 2H, $H_{2'}$+$H_{6'}$). ^{13}C NMR (100 MHz, $CDCl_3$): δ 13.6 (CH_3), 25.0 (CH_2–Se), 42.1 (CH_2), 55.9 (OCH_3), 100.9, 110.6, 112.4, 115.3, 129.4, 130.5, 131.4, 133.6, 138.0, 139.8, 156.4 (C_{aryl}), 168.4 (Ph-C═O), 175.3 (OH–C═O), 198.9 (Se–C═O). ^{77}Se NMR (76 MHz, $CDCl_3$): δ 591. HRMS *m/z*: calcd for $C_{21}H_{18}ClNO_5Se$ $[M + Na]^+$, 501.9931; found, 501.9913.

2-((2-(3-Benzoylphenyl)propanoyl)selenyl)acetic acid (**5a**). The title compound was synthesized from 2-(3-benzoylphenyl)propionic acid, oxalyl chloride, selenium, sodium borohydride and bromoacetic acid according to the general procedure described above. A white powder was obtained. Yield: 28%; mp: 59-61 °C. ^{1}H NMR (400 MHz, $CDCl_3$): δ 1.60 (d, $J = 7.1$ Hz, 3H, CH_3); 3.60 (d, $J = 5.0$ Hz, 2H, CH_2); 3.99 (q, $J =$ 7.1 Hz, 1H, CH); 7.49 (m, 3H, $H_{3'}$+$H_{4'}$+$H_{5'}$); 7.55 (dt, $J = 7.7$ and 1.5 Hz, 1H, H_6); 7.60 (m, 1H, H_5); 7.76 (m, 2H, H_2+H_4); 7.80 (m, 2H, $H_{2'}$+$H_{6'}$). ^{13}C NMR (100 MHz, $CDCl_3$): δ 18.0 (CH_3), 25.3 (CH_2), 57.3 (CH), 128.5, 129.0, 130.1, 130.3, 132.6, 132.8, 137.4, 138.3, 138.7 (C_{aryl}), 175.0 (OH–C═O), 196.4 (Ph-C═O), 201.6 (Se–C═O). ^{77}Se NMR (76 MHz, $CDCl_3$): δ 569. HRMS *m/z*: calcd for $C_{18}H_{16}O_4Se$ $[M + Na]^+$, 399.0106; found, 399.0106.

Methyl-2-((2-acetoxybenzoyl)selenyl)acetate (**1b**). The title compound was synthesized from *O*-acetylsalicyloyl chloride, selenium, sodium borohydride and methyl bromoacetate according to the general procedure described above. A yellow oil was obtained. Yield: 17%. ^{1}H NMR (400 MHz, $CDCl_3$): δ 2.38 (s, 3H, CH_3); 3.74 (s, 3H, OCH_3); 3.80 (s, 2H, CH_2); 7.16 (dd, $J = 8.1$ and 1.0 Hz, 1H, H_3); 7.35 (td, $J = 7.7$ and 1.1 Hz, 1H, H_5); 7.59 (td, $J = 7.7$ and 1.6 Hz, 1H, H_4); 7.91 (dd, $J = 7.9$ and 1.6 Hz, 1H, H_6). ^{13}C NMR (100 MHz, $CDCl_3$): δ 21.5 (CH_3), 25.9 (CH_2), 52.9 (OCH_3), 124.3, 126.5, 129.8, 130.9, 134.4, 147.9 (C_{aryl}), 169.2 (CH_3–C═O), 170.7 (CH_3O–C═O), 189.6 (Se–C═O). ^{77}Se NMR (76 MHz, $CDCl_3$): δ 583. HRMS *m/z*: calcd for $C_{12}H_{12}O_5Se$ $[M + Na]^+$, 338.9742; found, 338.9747.

Methyl-2-((2-hydroxybenzoyl)selenyl)acetate (**2b**). The title compound was synthesized from *O*-acetylsalicyloyl chloride, selenium, sodium borohydride and methyl bromoacetate according to the general procedure described above. An orange powder was obtained. Yield: 10%; mp: 56-57 °C. ^{1}H NMR (400 MHz, $CDCl_3$): δ 3.76 (s, 3H, OCH_3); 3.84 (s, 2H, CH_2); 6.95 (ddd, $J = 8.2$, 7.3 and 1.1 Hz, 1H, H_5); 6.99 (dd, $J =$ 8.4 and 1.0 Hz, 1H, H_3); 7.51 (ddd, $J = 8.6$, 7.3 and 1.5 Hz, 1H, H_4); 7.73 (dd, $J = 8.1$ and 1.5 Hz, 1H, H_6); 10.41 (s, 1H, OH). ^{13}C NMR (100 MHz, $CDCl_3$): δ 25.2 (CH_2), 53.1 (OCH_3), 118.5, 120.1, 121.7, 129.9, 136.7, 158.5 (C_{aryl}), 170.4 (CH_3O–C═O), 197.9 (Se–C═O). ^{77}Se NMR (76 MHz, $CDCl_3$): δ 536. HRMS *m/z*: calcd for $C_{10}H_{10}O_4Se$ $[M + Na]^+$, 296.9636; found, 296.9625.

*Methyl-(S)-2-((2-(6-methoxynaphthalen-*2-yl*)propanoyl)selenyl)acetate* (**3b**). The title compound was synthesized from (*S*)-2-(6-methoxy-2-naphthyl)propionyl chloride, selenium, sodium borohydride and methyl bromoacetate according to the general procedure described above. A white powder was obtained. Yield: 55%; mp: 37-38 °C. ^{1}H NMR (400 MHz, $CDCl_3$): δ 1.64 (d, $J = 7.1$ Hz, 3H, CH_3); 3.56 (d, $J = 12$ Hz, 2H, CH_2); 3.66 (s, 3H, OCH_3); 3.92 (s, 3H, OCH_3-Ph); 4.02 (q, $J = 7.1$ Hz, 1H, CH); 7.13 (s, 1H, H_5); 7.17 (d, $J = 8.9$, 1H, H_7); 7.36 (d, $J = 8.2$ Hz, 1H, H_8); 7.73 (m, 3H, H_1+H_3+H_4). ^{13}C NMR (100 MHz, $CDCl_3$): δ 17.9 (CH_3), 25.5 (CH_2), 52.7 (OCH_3), 55.5 (OCH_3-Ph), 57.4 (CH), 105.8, 119.4, 126.8, 127.6, 127.9, 129.0, 129.6, 133.4, 134.4, 158.2 (C_{aryl}), 170.9 (CH_3O–C═O), 202.3 (Se–C═O). ^{77}Se NMR (76 MHz, $CDCl_3$): δ 563. HRMS *m/z*: calcd for $C_{17}H_{18}O_4Se$ $[M + Na]^+$, 389.0262; found, 389.0249.

*Methyl-2-((2-(1-(4-chlorobenzoyl)-5-methoxy-2-methyl-1H-indol-*3-yl*) acetyl)selenyl)acetate* (**4b**). The title compound was synthesized from 1-(4-chlorobenzoyl)-5-methoxy-2-methyl-3-indoleacetic acid, oxalyl chloride, selenium, sodium borohydride and methyl bromoacetate according to the general procedure described above. A yellow powder was obtained. Yield: 49%; mp: 66-67 °C. ^{1}H NMR (400 MHz, $CDCl_3$): δ 2.41 (s, 3H, CH_3); 3.60 (s, 2H, CH_2–Se); 3.68 (s, 3H, OCH_3); 3.83 (s, 3H, OCH_3-Ph); 3.90 (s, 2H, CH_2); 6.70 (dd, $J = 9.0$ and 2.5 Hz, 1H, H_6); 6.88 (d, $J = 2.4$ Hz, 1H, H_4); 6.90 (d, $J = 9.1$ Hz, 1H, H_7); 7.49 (d, $J = 8.6$ Hz, 2H, $H_{3'}$+$H_{5'}$); 7.68 (d, $J = 8.6$ Hz, 2H, $H_{2'}$+$H_{6'}$). ^{13}C NMR (100 MHz, $CDCl_3$): δ 13.7 (CH_3), 25.3 (CH_2–Se), 42.2 (CH_2), 52.8 (OCH_3), 55.9 (OCH_3-Ph), 101.1, 110.8, 112.3, 115.2, 129.4, 130.6, 131.0, 131.4, 133.7, 137.9, 139.8, 156.4 (C_{aryl}), 168.4 (Ph-C═O), 170.8 (CH_3O–C═O), 198.6 (Se–C═O). ^{77}Se NMR (76 MHz, $CDCl_3$): δ 582. HRMS *m/z*: calcd for $C_{22}H_{20}ClNO_5Se$ $[M + Na]^+$, 516.0087; found, 516.0083.

Methyl-2-((2-(3-benzoylphenyl)propanoyl)selenyl)acetate (**5b**). The title compound was synthesized from 2-(3-benzoylphenyl)propionic acid, oxalyl chloride, selenium, sodium borohydride and methyl bromoacetate according to the general procedure described above. A yellow oil was obtained. Yield: 13%. ^{1}H NMR (400 MHz, $CDCl_3$): δ 1.59 (d, $J =$ 7.1 Hz, 3H, CH_3); 3.61 (d, $J = 6.5$ Hz, 2H, CH_2); 3.68 (s, 3H, OCH_3); 3.98 (q, $J = 7.1$ Hz, 1H, CH); 7.49 (m, 3H, $H_{3'}$+$H_{4'}$+$H_{5'}$); 7.55 (dt, $J = 7.7$ and 1.5 Hz, 1H, H_6); 7.60 (td, $J = 7.4$ and 1.3 Hz, 1H, H_5); 7.75 (m, 2H, H_2+H_4); 7.81 (m, 2H, $H_{2'}$+$H_{6'}$). ^{13}C NMR (100 MHz, $CDCl_3$): δ 18.0 (CH_3), 25.6 (CH_2), 52.8 (OCH_3), 57.3 (CH), 128.5, 129.0, 130.0, 130.2, 130.3, 132.5, 132.8, 137.5, 138.2, 138.8 (C_{aryl}), 170.7 (CH_3O–C═O), 196.4 (Ph-C═O), 201.4 (Se–C═O). ^{77}Se NMR (76 MHz, $CDCl_3$): δ 561. HRMS *m/z*: calcd for $C_{19}H_{18}O_4Se$ $[M + Na]^+$, 413.0262; found, 413.0266.

2-(((2-(Methylamino)-2-oxoethyl)selenyl)carbonyl)phenyl acetate (**1c**). The title compound was synthesized from *O*-acetylsalicyloyl chloride, selenium, sodium borohydride and 2-bromo-N-methylacetamide according to the general procedure described above. A white powder was obtained. Yield: 10%; mp: 111-112 °C. ^{1}H NMR (400 MHz, $CDCl_3$): δ 2.37 (s, 3H, CH_3); 2.81 (d, $J = 4.9$ Hz, 3H, NCH_3); 3.62 (s, 2H, CH_2); 6.24

(s, 1H, NH); 7.17 (dd, $J = 8.1$ and 1.0 Hz, 1H, H_3); 7.37 (td, $J = 7.7$ and 1.1 Hz, 1H, H_5); 7.62 (td, $J = 7.9$ and 1.6 Hz, 1H, H_4); 7.91 (dd, $J = 7.9$ and 1.6 Hz, 1H, H_6). ^{13}C NMR (100 MHz, $CDCl_3$): δ 21.5 (CH_3), 26.9 (CH_2), 27.9 (NCH_3), 124.2, 126.6, 129.7, 130.9, 134.7, 147.8 (C_{aryl}), 169.2 (CH_3–C═O), 170.4 (NH–C═O), 192.9 (Se–C═O). ^{77}Se NMR (76 MHz, $CDCl_3$): δ 606. HRMS *m/z*: calcd for $C_{12}H_{13}NO_4Se$ $[M + Na]^+$, 337.9902; found, 337.9907.

Se-(2-(Methylamino)-2-oxoethyl)-2-hydroxybenzoselenoate (**2c**). The title compound was synthesized from *O*-acetylsalicyloyl chloride, selenium, sodium borohydride and 2-bromo-N-methylacetamide according to the general procedure described above. A yellow powder was obtained. Yield: 5%; mp: 87-90 °C. ^{1}H NMR (400 MHz, $CDCl_3$): δ 2.83 (d, $J = 4.9$ Hz, 3H, NCH_3); 3.69 (s, 2H, CH_2); 6.28 (s, 1H, NH); 6.96 (t, $J = 7.7$ Hz, 1H, H_5); 7.00 (d, $J = 8.5$ Hz, 1H, H_3); 7.53 (m, 1H, H_4); 7.75 (dd, $J = 8.1$ and 1.3 Hz, 1H, H_6); 10.43 (s, 1H, OH). ^{13}C NMR (100 MHz, $CDCl_3$): δ 27.0 (CH_2), 27.1 (NCH_3), 118.5, 120.2, 121.8, 130.0, 137.1, 158.5 (C_{aryl}), 170.2 (NH–C═O), 200.5 (Se–C═O). ^{77}Se NMR (76 MHz, $CDCl_3$): δ 557. HRMS *m/z*: calcd for $C_{10}H_{11}NO_3Se$ $[M + Na]^+$, 295.9796; found, 295.9787.

Se-(2-(Methylamino)-2-oxoethyl)-(S)-2-(6-methoxynaphthalen-2-yl*) propaneselenoate* (**3c**). The title compound was synthesized from (*S*)-2-(6-methoxy-2-naphthyl)propionyl chloride, selenium, sodium borohydride and 2-bromo-N-methylacetamide according to the general procedure described above. A white powder was obtained. Yield: 10%; mp: 74-76 °C. ^{1}H NMR (400 MHz, $CDCl_3$): δ 1.64 (d, $J = 7.1$ Hz, 3H, CH_3); 2.73 (d, $J = 4.9$ Hz, 3H, NCH_3); 3.39 (d, $J = 2.5$ Hz, 2H, CH_2); 3.92 (s, 3H, OCH_3); 4.05 (q, $J = 7.1$ Hz, 1H, CH); 6.07 (s, 1H, NH); 7.13 (s, 1H, H_5); 7.17 (dd, $J = 8.9$ and 2.5 Hz, 1H, H_7); 7.35 (dd, $J = 8.5$ and 1.9 Hz, 1H, H_8); 7.69 (s, 1H, H_1); 7.73 (dd, $J = 8.7$ and 2.7 Hz, 2H, H_3+H_4). ^{13}C NMR (100 MHz, $CDCl_3$): δ 17.9 (CH_3), 26.8 (CH_2), 27.5 (NCH_3), 55.5 (OCH_3), 57.6 (CH), 105.8, 119.5, 126.6, 127.6, 127.7, 129.0, 129.5, 133.3, 134.4, 158.2 (C_{aryl}), 170.5 (NH–C═O), 205.7 (Se–C═O). ^{77}Se NMR (76 MHz, $CDCl_3$): δ 583. HRMS *m/z*: calcd for $C_{17}H_{19}NO_3Se$ $[M + Na]^+$, 388.0422; found, 388.0443.

Se-(2-(Methylamino)-2-oxoethyl)-2-(1-(4-chlorobenzoyl)-5-methoxy-2-methyl-1H-indol-3-yl*)ethaneselenoate* (**4c**). The title compound was synthesized from 1-(4-chlorobenzoyl)-5-methoxy-2-methyl-3-indoleacetic acid, oxalyl chloride, selenium, sodium borohydride and 2-bromo-N-methylacetamide according to the general procedure described above. A white powder was obtained. Yield: 74%; mp: 98-100 °C. ^{1}H NMR (400 MHz, $CDCl_3$): δ 2.40 (s, 3H, CH_3); 2.76 (d, $J = 4.9$ Hz, 3H, NCH_3); 3.42 (s, 2H, CH_2–Se); 3.83 (s, 3H, OCH_3); 3.91 (s, 2H, CH_2); 6.09 (s, 1H, NH); 6.70 (dd, $J = 9.0$ and 2.5 Hz, 1H, H_6); 6.86 (d, $J = 2.5$ Hz, 1H, H_4); 6.89 (d, $J = 9.0$ Hz, 1H, H_7); 7.49 (d, $J = 8.5$ Hz, 2H, $H_{3'}$+$H_{5'}$); 7.67 (d, $J = 8.5$ Hz, 2H, $H_{2'}$+$H_{6'}$). ^{13}C NMR (100 MHz, $CDCl_3$): δ 13.6 (CH_3), 26.9 (CH_2–Se), 27.4 (NCH_3), 42.5 (CH_2), 55.9 (OCH_3), 101.1, 110.7, 112.1, 115.3, 129.4, 130.4, 131.0, 131.4, 133.6, 137.8, 139.8, 156.4 (C_{aryl}), 168.4 (Ph-C═O), 170.5 (NH–C═O), 201.9 (Se–C═O). ^{77}Se NMR (76 MHz, $CDCl_3$): δ 603. HRMS *m/z*: calcd for $C_{22}H_{21}ClN_2O_4Se$ $[M + Na]^+$, 515.0247; found, 515.0244.

Se-(2-(Methylamino)-2-oxoethyl)-2-(3-benzoylphenyl)propane-selenoate (**5c**). The title compound was synthesized from 2-(3-benzoylphenyl)propionic acid, oxalyl chloride, selenium, sodium borohydride and 2-bromo-N-methylacetamide according to the general procedure described above. A pink powder was obtained. Yield: 20%; mp: 61-63 °C. ^{1}H NMR (400 MHz, $CDCl_3$): δ 1.60 (d, $J = 7.1$ Hz, 3H, CH_3); 2.76 (d, $J = 4.9$ Hz, 3H, CH_3); 3.43 (s, 2H, CH_2); 4.01 (q, $J = 7.1$ Hz, 1H, CH); 6.08 (s, 1H, NH); 7.49 (m, 3H, $H_{3'}$+$H_{4'}$+$H_{5'}$); 7.53 (dt, $J = 7.8$ and 1.4 Hz, 1H, H_6); 7.61 (t, $J = 7.4$ Hz, 1H, H_5); 7.74 (m, 2H, H_2+H_4); 7.80 (m, 2H, $H_{2'}$+$H_{6'}$). ^{13}C NMR (100 MHz, $CDCl_3$): δ 17.9 (CH_3), 26.7 (CH_2), 27.6 (NCH_3), 57.3 (CH), 128.4, 128.9, 129.9, 130.1, 132.3, 132.7, 137.3, 138.2, 138.7 (C_{aryl}), 170.2 (NH–C═O), 196.2 (Ph-C═O), 204.7 (Se–C═O). ^{77}Se NMR (76 MHz, $CDCl_3$): δ 584. HRMS *m/z*: calcd for $C_{19}H_{19}NO_3Se$ $[M + Na]^+$, 412.0422; found, 412.0437.

2-(((Cyanomethyl)selenyl)carbonyl)phenyl acetate (**1d**). The title compound was synthesized from *O*-acetylsalicyloyl chloride, selenium, sodium borohydride and bromoacetonitrile according to the general procedure described above. A pink powder was obtained. Yield: 56%; mp: 60-61 °C. ^{1}H NMR (400 MHz, $CDCl_3$): δ 2.41 (s, 3H, CH_3); 3.64 (s, 2H, CH_2); 7.21 (dd, $J = 8.2$ and 0.9 Hz, 1H, H_3); 7.38 (td, $J = 7.7$ and 0.9 Hz, 1H, H_5); 7.65 (td, $J = 7.8$ and 1.6 Hz, 1H, H_4); 7.88 (dd, $J = 7.6$ and 1.6 Hz, 1H, H_6). ^{13}C NMR (100 MHz, $CDCl_3$): δ 6.0 (CH_2), 21.6 (CH_3), 117.3 (CN), 124.4, 126.7, 129.7, 129.8, 135.1, 148.4 (C_{aryl}), 168.9 (CH_3–C═O), 187.5 (Se–C═O). ^{77}Se NMR (76 MHz, $CDCl_3$): δ 628. HRMS *m/z*: calcd for $C_{11}H_9NO_3Se$ $[M + Na]^+$, 305.9640; found, 305.9644.

Se-(Cyanomethyl)-2-hydroxybenzoselenoate (**2d**). The title compound was synthesized from *O*-acetylsalicyloyl chloride, selenium, sodium borohydride and bromoacetonitrile according to the general procedure described above. A yellow powder was obtained. Yield: 8%; mp: 54-56 °C. ^{1}H NMR (400 MHz, $CDCl_3$): δ 3.70 (s, 2H, CH_2); 6.99 (t, $J = 7.6$ Hz, 1H, H_5); 7.03 (d, $J = 8.4$ Hz, 1H, H_3); 7.56 (t, $J = 8.5$ Hz, 1H, H_4); 7.62 (dd, $J = 8.1$ and 1.3 Hz, 1H, H_6); 10.14 (s, 1H, OH). ^{13}C NMR (100 MHz, $CDCl_3$): δ 5.5 (CH_2), 117.0 (CN), 118.7, 120.4, 121.1, 129.6, 137.4, 158.7 (C_{aryl}), 195.5 (Se–C═O). ^{77}Se NMR (76 MHz, $CDCl_3$): δ 582. HRMS *m/z*: calcd for $C_9H_7NO_2Se$ $[M + Na]^+$, 263.9534; found, 263.9538.

Se-(Cyanomethyl)-(S)-2-(6-methoxynaphthalen-2-yl*)propaneselenoate* (**3d**). The title compound was synthesized from (*S*)-2-(6-methoxy-2-naphthyl)propionyl chloride, selenium, sodium borohydride and bromoacetonitrile according to the general procedure described above. A white powder was obtained. Yield: 74%; mp: 73-74 °C. ^{1}H NMR (400 MHz, $CDCl_3$): δ 1.67 (d, $J = 7.2$ Hz, 3H, CH_3); 3.38 (d, $J = 7.0$ Hz, 2H, CH_2); 3.93 (s, 3H, OCH_3); 4.02 (q, $J = 7.1$ Hz, 1H, CH); 7.15 (d, $J = 2.5$ Hz, 1H, H_5); 7.20 (dd, $J = 8.9$ and 2.5 Hz, 1H, H_7); 7.34 (dd, $J = 8.5$ and 1.9 Hz, 1H, H_8); 7.72 (s, 1H, H_1), 7.75 (m, 2H, H_3+H_4). ^{13}C NMR (100 MHz, $CDCl_3$): δ 5.6 (CH_2), 17.6 (CH_3), 55.5 (OCH_3), 57.2 (CH), 105.8 (C_{aryl}), 117.4 (CN), 119.7, 126.8, 127.8, 128.3, 128.9, 129.6, 132.4, 134.6, 158.4 (C_{aryl}), 201.0 (Se–C═O). ^{77}Se NMR (76 MHz, $CDCl_3$): δ 612. HRMS *m/z*: calcd for $C_{16}H_{15}NO_2Se$ $[M + Na]^+$, 356.0160; found, 356.0163.

Se-(Cyanomethyl)-2-(1-(4-chlorobenzoyl)-5-methoxy-2-methyl-1H-indol-3-yl*)ethaneselenoate* (**4d**). The title compound was synthesized from 1-(4-chlorobenzoyl)-5-methoxy-2-methyl-3-indoleacetic acid, oxalyl chloride, selenium, sodium borohydride and bromoacetonitrile according to the general procedure described above. A yellow powder was obtained. Yield: 54%; mp: 58-59 °C. ^{1}H NMR (400 MHz, $CDCl_3$): δ 2.43 (s, 3H, CH_3); 3.41 (s, 2H, CH_2); 3.84 (s, 3H, OCH_3); 3.93 (s, 2H, CH_2); 6.73 (dd, $J = 9.0$ and 2.5 Hz, 1H, H_6); 6.84 (d, $J = 2.4$ Hz, 1H, H_4); 6.90 (d, $J = 9.0$ Hz, 1H, H_7); 7.50 (d, $J = 8.5$ Hz, 2H, $H_{3'}$+$H_{5'}$); 7.68 (d, $J = 8.5$ Hz, 2H, $H_{2'}$+$H_{6'}$). ^{13}C NMR (100 MHz, $CDCl_3$): δ 5.3 (CH_2–Se), 13.6 (CH_3), 41.7 (CH_2), 55.9 (OCH_3), 100.7, 109.7, 112.6, 115.3 (C_{aryl}), 117.3 (CN), 129.5, 130.3, 131.0, 131.4, 133.4, 138.6, 140.0, 156.5 (C_{aryl}), 168.4 (Ph-C═O), 197.7 (Se–C═O). ^{77}Se NMR (76 MHz, $CDCl_3$): δ 636. HRMS *m/z*: calcd for $C_{21}H_{17}ClN_2O_3Se$ $[M + Na]^+$, 482.9985; found, 482.9981.

Se-(Cyanomethyl)-2-(3-benzoylphenyl)propaneselenoate (**5d**). The title compound was synthesized from 2-(3-benzoylphenyl)propionic acid, oxalyl chloride, selenium, sodium borohydride and bromoacetonitrile according to the general procedure described above. A white powder was obtained. Yield: 47%; mp: 60-61 °C. ^{1}H NMR (400 MHz, $CDCl_3$): δ 1.63 (d, $J = 7.2$ Hz, 3H, CH_3); 3.44 (d, $J = 2.6$ Hz, 2H, CH_2); 3.99 (q, $J = 7.1$ Hz, 1H, CH); 7.52 (m, 4H, H_6+$H_{3'}$+$H_{4'}$+$H_{5'}$); 7.62 (t, $J = 7.3$ Hz, 1H, H_5); 7.79 (m, 4H, H_2+H_4+$H_{2'}$+$H_{6'}$). ^{13}C NMR (100 MHz, $CDCl_3$): δ 5.7 (CH_2), 17.7 (CH_3), 57.2 (CH), 117.2 (CN), 128.6, 129.2, 130.2, 130.4, 130.5, 132.6, 132.9, 137.3, 137.9, 138.5 (C_{aryl}), 196.2 (Ph-C═O), 199.9 (Se–C═O). ^{77}Se NMR (76 MHz, $CDCl_3$): δ 610. HRMS *m/z*: calcd for $C_{18}H_{15}NO_2Se$ $[M + Na]^+$, 380.0160; found, 380.0163.

2-(((2-Cyanoethyl)selenyl)carbonyl)phenyl acetate (**1e**). The title compound was synthesized from *O*-acetylsalicyloyl chloride, selenium, sodium borohydride and 3-bromopropionitrile according to the general procedure described above. A yellow oil was obtained. Yield: 26%. ^{1}H

NMR (400 MHz, $CDCl_3$): δ 2.37 (s, 3H, CH_3); 2.83 (t, $J = 7.1$ Hz, 2H, CH_2–CN); 3.21 (t, $J = 7.1$ Hz, 2H, CH_2–Se); 7.15 (d, $J = 8.1$ Hz, 1H, H_3); 7.36 (t, $J = 7.7$ Hz, 1H, H_5); 7.60 (t, $J = 7.9$ Hz, 1H, H_4); 7.89 (d, $J = 7.8$ Hz, 1H, H_6). ^{13}C NMR (100 MHz, $CDCl_3$): δ 19.4 (CH_2–CN), 20.3 (CH_2–Se), 21.4 (CH_3), 118.8 (CN), 124.3, 126.6, 129.9, 131.0, 134.5, 147.6 (C_{aryl}), 169.3 (CH_3–C═O), 190.8 (Se–C═O). ^{77}Se NMR (76 MHz, $CDCl_3$): δ 585. HRMS *m/z*: calcd for $C_{12}H_{11}NO_3Se$ $[M + Na]^+$, 319.9796; found, 319.9745.

Se-(2-Cyanoethyl)2-hydroxybenzoselenoate (**2e**). The title compound was synthesized from *O*-acetylsalicyloyl chloride, selenium, sodium borohydride and 3-bromopropionitrile according to the general procedure described above. A white powder was obtained. Yield: 12%; mp: 81-83 °C. ^{1}H NMR (400 MHz, $CDCl_3$): δ 2.88 (t, $J = 7.1$ Hz, 2H, CH_2–CN); 3.28 (t, $J = 7.1$ Hz, 2H, CH_2–Se); 6.97 (m, 2H, H_3+H_5); 7.51 (td, $J = 8.3$ and 1.1 Hz, 1H, H_4); 7.72 (dd, $J = 8.0$ and 1.1 Hz, 1H, H_6); 10.43 (s, 1H, OH). ^{13}C NMR (100 MHz, $CDCl_3$): δ 19.5 (CH_2–CN), 19.8 (CH_2–Se), 118.5 (C_{aryl}), 118.6 (CN), 120.1, 121.9, 130.0, 136.9, 158.5 (C_{aryl}), 198.9 (Se–C═O). ^{77}Se NMR (76 MHz, $CDCl_3$): δ 538. HRMS *m/z*: calcd for $C_{10}H_9NO_2Se$ $[M + Na]^+$, 277.9691; found, 277.9695.

Se-(2-Cyanoethyl)(S)-2-(6-methoxynaphthalen-2-yl*)propaneselenoate* (**3e**). The title compound was synthesized from (*S*)-2-(6-methoxy-2-naphthyl)propionyl chloride, selenium, sodium borohydride and 3-bromopropionitrile according to the general procedure described above. A yellow powder was obtained. Yield: 71%; mp: 68-70 °C. ^{1}H NMR (400 MHz, $CDCl_3$): δ 1.63 (d, $J = 7.1$ Hz, 3H, CH_3); 2.69 (t, $J = 7.1$ Hz, 2H, CH_2–CN); 2.99 (td, $J = 7.2$ and 3.0 Hz, 2H, CH_2–Se); 3.92 (s, 3H, OCH_3); 4.02 (q, $J = 7.1$ Hz, 1H, CH); 7.14 (d, $J = 2.4$ Hz, 1H, H_5); 7.17 (dd, $J = 8.9$ and 2.4 Hz, 1H, H_7); 7.35 (dd, $J = 8.5$ and 1.5 Hz, 1H, H_8); 7.69 (s, 1H, H_1); 7.74 (d, $J = 8.7$ Hz, 2H, H_3+H_4). ^{13}C NMR (100 MHz, $CDCl_3$): δ 17.9 (CH_3), 19.4 (CH_2–CN), 19.7 (CH_2–Se), 55.5 (OCH_3), 57.9 (CH), 105.8 (C_{aryl}), 118.7 (CN), 119.5, 126.7, 127.6, 127.7, 129.0, 129.5, 133.4, 134.4, 158.2 (C_{aryl}), 203.3 (Se–C═O). ^{77}Se NMR (76 MHz, $CDCl_3$): δ 563. HRMS *m/z*: calcd for $C_{17}H_{17}NO_2Se$ $[M + Na]^+$, 370.0317; found, 370.0318.

Se-(2-Cyanoethyl)2-(1-(4-chlorobenzoyl)-5-methoxy-2-methyl-1H-indol-3-yl*)ethane selenoate* (**4e**). The title compound was synthesized from 1-(4-chlorobenzoyl)-5-methoxy-2-methyl-3-indoleacetic acid, oxalyl chloride, selenium, sodium borohydride and 3-bromopropionitrile according to the general procedure described above. A white powder was obtained. Yield: 78%; mp: 106-108 °C. ^{1}H NMR (400 MHz, $CDCl_3$): δ 2.40 (s, 3H, CH_3); 2.73 (t, $J = 7.1$ Hz, 2H, CH_2–CN); 3.02 (t, $J = 7.1$ Hz, 2H, CH_2–Se); 3.84 (s, 3H, OCH_3); 3.90 (s, 2H, CH_2); 6.71 (dd, $J = 9.0$ and 2.4 Hz, 1H, H_6); 6.88 (d, $J = 2.4$ Hz, 1H, H_4); 6.91 (d, $J = 9.0$ Hz, 1H, H_7); 7.49 (d, $J = 8.5$ Hz, 2H, $H_{3'}$+$H_{5'}$); 7.68 (d, $J = 8.5$ Hz, 2H, $H_{2'}$+$H_{6'}$). ^{13}C NMR (100 MHz, $CDCl_3$): δ 13.7 (CH_3), 19.4 (CH_2–CN), 19.6 (CH_2–Se), 42.7 (CH_2), 55.9 (OCH_3), 101.0, 110.8, 112.3, 115.2 (C_{aryl}), 118.6 (CN), 129.4, 130.5, 131.0, 131.4, 133.7, 137.7, 139.8, 156.4 (C_{aryl}), 168.4 (Ph-C═O), 199.5 (Se–C═O). ^{77}Se NMR (76 MHz, $CDCl_3$): δ 581. HRMS *m/z*: calcd for $C_{22}H_{19}ClN_2O_3Se$ $[M + Na]^+$, 497.0142; found, 497.0144.

Se-(2-Cyanoethyl)2-(3-benzoylphenyl)propaneselenoate (**5e**). The title compound was synthesized from 2-(3-benzoylphenyl)propionic acid, oxalyl chloride, selenium, sodium borohydride and 3-bromopropionitrile according to the general procedure described above. A white powder was obtained. Yield: 35%; mp: 51-53 °C. ^{1}H NMR (400 MHz, $CDCl_3$): δ 1.59 (d, $J = 7.1$ Hz, 3H, CH_3); 2.73 (t, $J = 7.1$ Hz, 2H, CH_2–CN); 3.04 (t, $J = 7.3$ Hz, 2H, CH_2–Se); 3.98 (q, $J = 7.1$ Hz, 1H, CH); 7.51 (m, 4H, H_6+$H_{3'}$+$H_{4'}$+$H_{5'}$); 7.61 (t, $J = 7.4$ Hz, 1H, H_5); 7.75 (m, 2H, H_2+H_4); 7.81 (d, $J = 7.3$ Hz, 2H, $H_{2'}$+$H_{6'}$). ^{13}C NMR (100 MHz, $CDCl_3$): δ 18.0 (CH_3), 19.4 (CH_2–CN), 20.0 (CH_2–Se), 57.7 (CH), 118.6 (CN), 128.5, 129.0, 130.0, 130.1, 130.2, 132.4, 132.8, 137.4, 138.3, 138.8 (C_{aryl}), 196.4 (Ph-C═O), 202.5 (Se–C═O). ^{77}Se NMR (76 MHz, $CDCl_3$): δ 563. HRMS *m/z*: calcd for $C_{19}H_{17}NO_2Se$ $[M + Na]^+$, 394.0317; found, 394.0367.

4.2. Solubility and stability studies

4.2.1. Determination of the aqueous solubility

The solubility of selected Se-NSAID derivatives in aqueous medium was evaluated with both *in silico* and *in vitro* methods. The aqueous solubility *in silico* was determined with the computational programs SwissADME [77] and OSIRIS [78]. Experimental solubility was carried out by adding an excess of compound to a solution of 0.5 mL in D_2O containing 4 mg of dimethyl sulfone as the internal standard. The suspension was analyzed by ^{1}H NMR. The quantitative determination was based on the premise that an integrated signal is proportional to the molar concentration [79]. Thus, the solubility values were obtained considering the ratio between the area of the peaks belonging to the dimethyl sulfone and the methoxy group (**4a** and **3e**), or one aryl hydrogen (**4b**, **4d**, and **4e**). ChemDraw software was used to determine the pK_a and ClogP values of the selected compounds.

4.2.2. Hydrolysis study

A hydrolysis study was performed for compounds **4a** and **4d** using q-^{1}H NMR. Briefly, each compound was dissolved in DMSO-d_6 containing 10% (*v/v*) of D_2O, and the ^{1}H NMR spectra were recorded at different time points for 48 h. The results are expressed as the percentage of hydrolysis and was calculated tracking the appearance of a new signal close to the signal corresponding to the aryl hydrogen H_7 for compound **4a**, or to the methyl group for compound **4d**.

4.2.3. Stability in gastrointestinal fluids

Simulated gastric and intestinal fluids were prepared according to USP specifications with either pepsin (3.2 mg/mL) or pancreatin (10 mg/mL), respectively. Stock solutions of compounds **4a** and **4d** dissolved in an organic solvent were added to preheated fluids placed in a 37 °C water bath. At predetermined time points, 500 μL of sample were picked up and deproteinized with 500 μL of acetonitrile. Samples were filtered before HPLC analysis. An HPLC/UV-DAD (HP 1100, Agilent Technologies, Santa Clara, CA, USA) equipped with a C18 column (Gemini 110A, 100 × 4.6 mm, 5 μm particle size) from Phenomenex (Phenomenex, Torrance, CA, USA) was used. The mobile phase was a mixture of acetonitrile/water (50:50) flushed with a flow rate of 1 mL/min. The injection volume was 50 μL for all the samples. UV-DAD detection was established at 254 nm. The RD was used to estimate the amount of degraded compound in SGF and SIF media and was calculated with the following formula: RD (%) = $[(C_i - C_f)/C_i] \times 100$, wherein C_i and is the amount of compound at the zero-time point, and C_f is the amount of compound at the end of the incubation for each time point measured [80].

4.3. Biology

4.3.1. Cell culture conditions

The cell lines were obtained from the American Type Culture Collection (ATCC). All the cancer cell lines (HT-54, DU-145, HT-29, MCF-7, T-47D, MDA-MB-231, H1299 and A549) and the non-tumorigenic cells (184B5 and BEAS-2B) were maintained in RPMI 1640 medium (Gibco), supplemented with 10% fetal bovine serum (FBS; Gibco) and 1% antibiotics (10.00 units/mL penicillin and 10.00 mg/mL streptomycin; Gibco). Cells were preserved in tissue culture flasks at 37 °C and 5% CO_2. Culture medium was replaced every three days.

4.3.2. Cell viability assay

Se-NSAID derivatives were dissolved in DMSO at a concentration of 0.01 M and serial dilutions were prepared. The cytotoxic and antiproliferative activities of each compound were initially tested at two different concentrations (10 and 50 μM) in HTB-54, DU-145, HT-29 and MCF-7 cells. Selected compounds were then tested at seven different concentrations ranging between 0.5 and 100 μM in HTB-54, DU-145, HT-29, MCF-7, 184B5, BEAS-2B, and additional breast (T-47D and

MDA-MB-231) or lung (H1299 and A549) cancer cells. A total of 1 x 10^4 cells were seeded per well in 96-well plates and then treated with either DMSO or increasing concentrations of the corresponding Se-derivative for 48 h. The effect of the compounds on cell viability was determined by the MTT (3-(4,5-dimethylthiazol-2-yl)-2,5-diphenyltetrazolium bromide) assay [66]. In brief, 20 μL of MTT (5 mg/mL) were added to each well 2.5 h prior to experiment termination. At the termination point, the medium was removed and the resultant formazan crystals were dissolved in 50 μL of DMSO. Absorbance was measured at 550 nm. IC_{50}, GI_{50}, TGI and LC_{50} values were calculated using OriginPro 8.5.1. software by nonlinear curve fitting. Selectivity indexes were calculated as the ratio of the IC_{50} values determined for the non-malignant and the tumoral cells in the breast (IC_{50} (184B5)/IC_{50} (MCF-7)) and lung (IC_{50} (BEAS-2B)/IC_{50} (HTB-54)) cell lines. Data were obtained from at least three independent experiments performed in triplicates.

4.3.3. NCI-60 analysis

Compounds **4a**, **4b**, **4d**, **3e** and **4e** were submitted to the NCI's DTP. The cytotoxicity profile of the selected compounds was evaluated in the NCI-60 human cancer cell line used to screen and identify test compounds that have an effect on cell proliferation [81] following the methodology available [82].

4.3.4. Trypan blue dye exclusion assay

This method has been traditionally used for cell viability analysis [83]. Briefly, MCF-7 and MDA-MB-231 cells were seeded in 12-well plates at a density of 6 x 10^4 cells per well for 24 h. Then, cells were treated with three serial concentrations (5, 10 and 25 μM) of compounds **4a** or **4d** for 24 h or 48 h. The cells were harvested after the end of the treatments and mixed with 1:2 volume of 0.4% Trypan Blue dye (Invitrogen, MA, USA). Cells were loaded over the hemocytometer and counted separately using a bright field microscope. Live and viable cells were unstained and presented a clear appearance, whereas dead or membrane-compromised cells were stained with the dye and appeared blue.

4.3.5. Apoptosis assays

Induction of apoptosis was analyzed using Annexin V & Dead Cell assay kit and Caspase 3/7 assay kit (EMD Millipore, Darmstadt, Germany). MCF-7 and MDA-MB-231 cells were seeded in 6-well plates at a density of 6 x 10^5 cells per well and treated either with DMSO (control) or with different concentrations of compounds **4a** and **4d** and incubated for 24 h. At the end of the treatment, cells were collected and treated with the respective dyes according to the manufacturer's protocol. For the Caspase 3/7 assay, cells were stained with 5 μL of Muse™ Caspase 3/7 working solution and incubated at 37 °C for 30 min. After incubation, 150 mL of Muse™ Caspase 7-AAD working solution was added and the samples were incubated for another 5 min in the dark at room temperature. For Annexin V assay, cells were stained with 100 μL pf Muse™ Annexin V & Dead Cell Reagent and incubated for 20 min at room temperature in the dark prior to analysis. Samples for both assays were further analyzed on a Muse™ Cell Analyzer (Merck Millipore, Darmstadt, Germany) using Muse™ 1.4 software.

4.3.6. Metabolite study

A solution of 100 mM of compound **4d** in acetonitrile was added to a solution of 100 mM phosphate buffer containing 0.5 mg/mL of human S9 fractions. The reaction mixture was pre-incubated for 5 min at 37 °C. Then the reaction was initiated with the addition of 10 μL of 20 mM NADPH. The control incubation was performed in the absence of microsomes. The incubations were carried out for 60 or 120 min maintaining a continuous stirring. At the end of the experiment, the reaction was terminated by the addition of 200 μL of ethyl acetate. The reaction mixture was centrifuged at 3000 rpm for 5 min and supernatants were analyzed independently. Samples (5 μL) were separated by reverse phase HPLC using a Prominence 20 UFLCXR system (Shimadzu, Columbia, MD) with a Waters (Milford, MA) BEH C18 column (100 mm × 2.1 mm 1.7 μm particle size) maintained at 55 °C and a 20 min aqueous acetonitrile gradient with a flow rate of 250 μL/min. Solvent A was HPLC grade water with 0.1% formic acid and Solvent B was HPLC grade acetonitrile with 0.1% formic acid. The initial conditions were 97% A and 3% B, increasing to 45% B at 10 min, and 75% B at 12 min where it was held at 75% B until 17.5 min before returning to the initial conditions. The eluate was delivered into a 5600 (QTOF) TripleTOF using a Duospray™ ion source (all Sciex, Framingham, MA). The capillary voltage was set at 5.5 kV in positive ion mode with a declustering potential of 80V. The mass spectrometer was operated with a 100 ms TOF scan from 50 to 1000 *m/z*, and 16 MS/MS product ion scans (100 ms) per duty cycle using a collision energy of 50V with a 20V spread. The line slopes were determined by plotting the peak area against incubation time.

4.3.7. Statistical analysis

Data were expressed as the mean ± SD (standard deviation) and experiments were performed at least thrice in triplicates unless otherwise specified. Non-linear curve regression analysis calculated by OriginPro 8.5.1. software was used to assess the IC_{50}, GI_{50}, TGI and LD_{50} values. The two-way analysis of variance (ANOVA) was used to calculate the statistical significance of differences comparing control and compounds or only treatments (**4a** and **4d**). Data were analyzed using GraphPad Prism version 8.0.1., and the statistically significant values (*p*-value) for ANOVA analysis were taken as $^{****}p < 0.0001$, $^{***}p < 0.001$, $^{**}p < 0.01$ and $^{*}p < 0.05$ or $^{\#\#\#\#}p < 0.0001$ and $^{\#\#}p < 0.01$.

Author contributions

Carmen Sanmartin and Daniel Plano devised the project and conceived the main conceptual ideas. Sandra Ramos-Inza synthesized and purified the compounds, performed all the biological experiments, and drafted the manuscript. Sandra Ramos-Inza, Ignacio Encío, Asif Raza, Arun K. Sharma and Daniel Plano analyzed the data. Arun K. Sharma, Carmen Sanmartin and Daniel Plano reviewed and edited the manuscript. All authors have given approval to the final version of the manuscript.

Declaration of competing interest

The authors declare the following financial interests/personal relationships which may be considered as potential competing interests: Daniel Plano reports financial support was provided by Plan de Investigación de la Universidad de Navarra (PIUNA 2018-19). Arun K. Sharma reports financial support was provided by Department of Pharmacology and Penn State Cancer Institute of the Penn State College of Medicine.

Data availability

Data will be made available on request.

Acknowledgments

This work was financially supported by the Plan de Investigación de la Universidad de Navarra, PIUNA (2018-19), and the Department of Pharmacology and Penn State Cancer Institute of the Penn State College of Medicine. Sandra Ramos-Inza also acknowledges the FPU program from the Spanish Ministry of Universities for a Ph.D. fellowship (FPU18/04679) and a mobility grant (EST19/00898). The authors wish to express their gratitude to Dr. Esther Moreno for providing the enzymes for the study of the stability in gastrointestinal fluids, and to Dr. Elena González-Peñas and Dr. Elena Lizarraga for their assistance with the HPLC measurements.

Appendix A. Supplementary data

Supplementary data to this article can be found online at https://doi.org/10.1016/j.ejmech.2022.114839.

Abbreviations

ASA	aspirin
ATCC	American Type Culture Collection
CNS	central nervous system
COX-1 and -2	cyclooxygenase-1 and -2
DTP	Developmental Therapeutics Program
FBS	fetal bovine serum
GP	growth percent
HER2	human epidermal growth factor receptor 2
HMGA2	human high-mobility group A2
HPLC	high-performance liquid chromatography
HRMS	high-resolution mass spectrometry
HS	hydrogen sulfide
Ind	indomethacin
Ket	ketoprofen
mp	melting point
MTT	3-(4,5-dimethylthiazol-2-yl)-2,5-diphenyltetrazolium bromide
Nap	naproxen
NCI	National Cancer Institute
Neu-1	neuraminidase-1
NF-κB	nuclear factor-kappaB
NMR	nuclear magnetic resonance
NO	nitric oxide
NSAIDs	nonsteroidal anti-inflammatory drugs
PS	phosphatidylserine
RD	relative difference
ROS	reactive oxygen species
Salic	salicylic acid
Se	selenium
SGF	simulated gastric fluid
SI	selectivity index
SIF	simulated intestinal fluid
TLC	thin-layer chromatography
TNF-α	tumor necrosis factor-alpha
TrxR	thioredoxin reductase

References

[1] S. Zappavigna, A.M. Cossu, A. Grimaldi, M. Bocchetti, G.A. Ferraro, G.F. Nicoletti, R. Filosa, M. Caraglia, Anti-inflammatory drugs as anticancer agents, Int. J. Mol. Sci. 21 (2020) 2605.

[2] P. Rao, E.E. Knaus, Evolution of nonsteroidal anti-inflammatory drugs (NSAIDs): cyclooxygenase (COX) inhibition and beyond, J. Pharm. Pharmaceut. Sci. 11 (2008) 81–110.

[3] S. Qin, C. Xu, S. Li, C. Yang, X. Sun, X. Wang, S.C. Tang, H. Ren, Indomethacin induces apoptosis in the EC109 esophageal cancer cell line by releasing second mitochondria-derived activator of caspase and activating caspase-3, Mol. Med. Rep. 11 (2015) 4694–4700.

[4] M. Garcia, R. Velez, C. Romagosa, B. Majem, N. Pedrola, M. Olivan, M. Rigau, M. Guiu, R.R. Gomis, J. Morote, J. Reventós, A. Doll, Cyclooxygenase-2 inhibitor suppresses tumour progression of prostate cancer bone metastases in nude mice, BJU Int. 113 (2014) E164–E177.

[5] V. Leidgens, C. Seliger, B. Jachnik, T. Welz, P. Leukel, A. Vollmann-Zwerenz, U. Bogdahn, M. Kreutz, O.M. Grauer, P. Hau, Ibuprofen and diclofenac restrict migration and proliferation of human glioma cells by distinct molecular mechanisms, PLoS One 10 (2015), e0140613.

[6] L.M. Lichtenberger, D. Fang, R.J. Bick, B.J. Poindexter, T. Phan, A.L. Bergeron, S. Pradhan, E.J. Dial, K.V. Vijayan, Unlocking aspirin's chemopreventive activity: role of irreversibly inhibiting platelet cyclooxygenase-1, Cancer Prev. Res. 10 (2017) 142–152.

[7] B. Trabert, E.M. Poole, E. White, K. Visvanathan, H.O. Adami, G.L. Anderson, T. M. Brasky, L.A. Brinton, R.T. Fortner, M. Gaudet, P. Hartge, J. Hoffman-Bolton, M. Jones, J.V. Lacey, S.C. Larsson, G.G. Mackenzie, L.J. Schouten, D.P. Sandler, K. O'Brien, A.V. Patel, U. Peters, A. Prizment, K. Robien, V.W. Setiawan, A. Swerdlow, P.A. van den Brandt, E. Weiderpass, L.R. Wilkens, A. Wolk, N. Wentzensen, S.S. Tworoger, Ovarian Cancer Cohort Consortium, Analgesic use and ovarian cancer risk: an analysis in the ovarian cancer cohort consortium, J. Natl. Cancer Inst. 111 (2019) 137–145.

[8] S. Ma, C. Guo, C. Sun, T. Han, H. Zhang, G. Qu, Y. Jiang, Q. Zhou, Y. Sun, Aspirin use and risk of breast cancer: a meta-analysis of observational studies from 1989 to 2019, Clin. Breast Cancer 21 (2021) 552–565.

[9] C.M. Sauer, D.T. Myran, C.E. Costentin, G. Zwisler, T. Safder, S. Papatheodorou, L. A. Mucci, Effect of long term aspirin use on the incidence of prostate cancer: a systematic review and meta-analysis, Crit. Rev. Oncol. Hematol. 132 (2018) 66–75.

[10] T.Y. Lee, Y.C. Hsu, H.C. Tseng, S.H. Yu, J.T. Lin, M.S. Wu, C.Y. Wu, Association of daily aspirin therapy with risk of hepatocellular carcinoma in patients with chronic hepatitis B, JAMA Intern. Med. 179 (2019) 633–640.

[11] T.Y. Lee, Y.C. Hsu, H.C. Tseng, J.T. Lin, M.S. Wu, C.Y. Wu, Association of daily aspirin therapy with hepatocellular carcinoma risk in patients with chronic hepatitis C virus infection, Clin. Gastroenterol. Hepatol. 18 (2020) 2784–2792, e7.

[12] T.G. Simon, A.S. Duberg, S. Aleman, R.T. Chung, A.T. Chan, J.F. Ludvigsson, Association of aspirin with hepatocellular carcinoma and liver-related mortality, N. Engl. J. Med. 382 (2020) 1018–1028.

[13] C.N. Kuo, J.J. Pan, Y.W. Huang, H.J. Tsai, W.C. Chang, Association between nonsteroidal anti-inflammatory drugs and colorectal cancer: a population-based case-control study, Cancer Epidemiol. Biomarkers Prev. 27 (2018) 737–745.

[14] A. Mohammed, N.S. Yarla, V. Madka, C.V. Rao, Clinically relevant anti-inflammatory agents for chemoprevention of colorectal cancer: new perspectives, Int. J. Mol. Sci. 19 (2018) 2332.

[15] J.C. Figueiredo, E.J. Jacobs, C.C. Newton, M.A. Guinter, W.G. Cance, P. T. Campbell, Associations of aspirin and non-aspirin non-steroidal anti-inflammatory drugs with colorectal cancer mortality after diagnosis, J. Natl. Cancer Inst. 113 (2021) 833–840.

[16] Y. Zhang, A.T. Chan, J.A. Meyerhardt, E.L. Giovannucci, Timing of aspirin use in colorectal cancer chemoprevention: a prospective cohort study, J. Natl. Cancer Inst. 113 (2021) 841–851.

[17] E.L. Amitay, P.R. Carr, L. Jansen, V. Walter, W. Roth, E. Herpel, M. Kloor, H. Bläker, J. Chang-Claude, H. Brenner, M. Hoffmeister, Association of aspirin and nonsteroidal anti-inflammatory drugs with colorectal cancer risk by molecular subtypes, J. Natl. Cancer Inst. 111 (2019) 475–483.

[18] Y.S. Zhao, S. Zhu, X.W. Li, F. Wang, F.L. Hu, D.D. Li, W.C. Zhang, X. Li, Association between NSAIDs use and breast cancer risk: a systematic review and meta-analysis, Breast Cancer Res. Treat. 117 (1) (2009) 141–150.

[19] A. Bardia, J.E. Olson, C.M. Vachon, D. Lazovich, R.A. Vierkant, A.H. Wang, P. J. Limburg, K.E. Anderson, J.R. Cerhan, Effect of aspirin and other NSAIDs on postmenopausal breast cancer incidence by hormone receptor status: results from a prospective cohort study, Breast Cancer Res. Treat. 126 (2011) 149–155.

[20] L. Lu, L. Shi, J. Zeng, Z. Wen, Aspirin as a potential modality for the chemoprevention of breast cancer: a dose-response meta-analysis of cohort studies from 857,831 participants, Oncotarget 8 (2017) 40389–40401.

[21] Y. Cao, A. Tan, Aspirin might reduce the incidence of breast cancer: an updated meta-analysis of 38 observational studies, Medicine (Baltim.) 99 (2020), e21917.

[22] J. Liu, F. Zheng, M. Yang, X. Wu, A. Liu, Effect of aspirin use on survival benefits of breast cancer patients: a meta-analysis, Medicine (Baltim.) 100 (2021), e26870.

[23] B. Takkouche, C. Regueira-Méndez, M. Etminan, Breast cancer and use of nonsteroidal anti-inflammatory drugs: a meta-analysis, J. Natl. Cancer Inst. 100 (2008) 1439–1447.

[24] C.H. Hung, Y.C. Lin, Y.H. Chang, Y.C. Lin, H.Y. Huang, W.J. Yeh, T.Y. Wu, M. F. Hou, The effect of NSAIDs exposure on breast cancer risk in female patients with autoimmune diseases, Eur. J. Cancer Prev. 28 (2019) 428–434.

[25] P.A. Thompson, C. Huang, J. Yang, B.C. Wertheim, D. Roe, X. Zhang, J. Ding, P. Chalasani, C. Preece, J. Martinez, H.S. Chow, A.T. Stopeck, Sulindac, a nonselective NSAID, reduces breast density in postmenopausal women with breast cancer treated with aromatase inhibitors, Clin. Cancer Res. 27 (2021) 5660–5668.

[26] R.D. Kehm, J.L. Hopper, E.M. John, K.A. Phillips, R.J. MacInnis, G.S. Dite, R. L. Milne, Y. Liao, N. Zeinomar, J.A. Knight, M.C. Southey, L. Vahdat, N. Kornhauser, T. Cigler, W.K. Chung, G.G. Giles, S.A. McLachlan, M. L. Friedlander, P.C. Weideman, G. Glendon, S. Nesci, I.L. Andrulis, S.S. Buys, M. B. Daly, M.B. Terry, Regular use of aspirin and other non-steroidal anti-inflammatory drugs and breast cancer risk for women at familial or genetic risk: a cohort study, Breast Cancer Res. 21 (2019) 52.

[27] C.A. Clarke, A.J. Canchola, L.M. Moy, S.L. Neuhausen, N.T. Chung, J.V. Lacey Jr., L. Bernstein, Regular and low-dose aspirin, other non-steroidal anti-inflammatory medications and prospective risk of HER2-defined breast cancer: the California Teachers Study, Breast Cancer Res. 19 (2017) 52.

[28] M. Cairat, A. Fournier, N. Murphy, C. Biessy, A. Scalbert, S. Rinaldi, A. Tjønneland, A. Olsen, K. Overvad, P. Arveux, M.C. Boutron-Ruault, C. Cadeau, R.T. Fortner, R. Kaaks, H. Boeing, K. Aleksandrova, P.H.M. Peeters, C.H. Van Gils, N. J. Wareham, K.T. Khaw, D. Aune, E. Riboli, M.J. Gunter, L. Dossus, Nonsteroidal anti-inflammatory drug use and breast cancer risk in a European prospective cohort study, Int. J. Cancer 143 (2018) 1688–1695.

[29] K.M. Knights, A.A. Mangoni, J.O. Miners, Defining the COX inhibitor selectivity of NSAIDs: implications for understanding toxicity, Expet Rev. Clin. Pharmacol. 3 (2010) 769–776.

[30] E. Yiannakopoulou, Aspirin and NSAIDs for breast cancer chemoprevention, Eur. J. Cancer Prev. 24 (2015) 416–421.

[31] F. Yan, Q. He, X. Hu, W. Li, K. Wei, L. Li, Y. Zhong, X. Ding, S. Xiang, J. Zhang, Direct regulation of caspase-3 by the transcription factor AP-2α is involved in aspirin-induced apoptosis in MDA-MB-453 breast cancer cells, Mol. Med. Rep. 7 (2013) 909–914.

[32] C. Huang, Y. Chen, H. Liu, J. Yang, X. Song, J. Zhao, N. He, C.J. Zhou, Y. Wang, C. Huang, Q. Dong, Celecoxib targets breast cancer stem cells by inhibiting the synthesis of prostaglandin E_2 and down-regulating the Wnt pathway activity, Oncotarget 8 (2017) 115254–115269.
[33] Y. Feng, L. Tao, G. Wang, Z. Li, M. Yang, W. He, X. Zhong, Y. Zhang, J. Yang, S. Cheung, F. McDonald, L. Chen, Aspirin inhibits prostaglandins to prevents colon tumor formation via down-regulating Wnt production, Eur. J. Pharmacol. 906 (2021), 174173.
[34] S.K. Bardaweel, L.A. Dahabiyeh, B.M. Akileh, D.D. Shalabi, A.K. AlHiary, J. Pawling, J.W. Dennis, A.M.A. Rahman, Molecular and metabolomic investigation of celecoxib antiproliferative activity in mono-and combination therapy against breast cancer cell models, Anti Cancer Agents Med. Chem. 22 (2021) 1611–1621.
[35] C.Y. Chang, J.R. Li, C.C. Wu, J.D. Wang, C.P. Yang, W.Y. Chen, W.Y. Wang, C. J. Chen, Indomethacin induced glioma apoptosis involving ceramide signals, Exp. Cell Res. 365 (2018) 66–77.
[36] T.I. Ekanem, W.L. Tsai, Y.H. Lin, W.Q. Tan, H.Y. Chang, T.C. Huang, H.Y. Chen, K. H. Lee, Identification of the effects of aspirin and sulindac sulfide on the inhibition of HMGA2-mediated oncogenic capacities in colorectal cancer, Molecules 25 (2020) 3826.
[37] B. Qorri, W. Harless, M.R. Szewczuk, Novel molecular mechanism of aspirin and celecoxib targeting mammalian neuraminidase-1 impedes epidermal growth factor receptor signaling axis and Induces apoptosis in pancreatic cancer cells, Drug Des. Dev. Ther. 14 (2020) 4149–4167.
[38] R. Fletcher, J. Tong, D. Risnik, B.J. Leibowitz, Y.J. Wang, F. Concha-Benavente, J. M. DeLiberty, D.B. Stolz, R.K. Pai, R.L. Ferris, R.E. Schoen, J. Yu, L. Zhang, Non-steroidal anti-inflammatory drugs induce immunogenic cell death in suppressing colorectal tumorigenesis, Oncogene 40 (2021) 2035–2050.
[39] X. Fu, T. Tan, P. Liu, Regulation of autophagy by non-steroidal anti-inflammatory drugs in cancer, Cancer Manag. Res. 12 (2020) 4595–4604.
[40] J.M. Scheiman, NSAID-induced gastrointestinal injury: a focused update for clinicians, J. Clin. Gastroenterol. 50 (2016) 5–10.
[41] P. Gurbel, U. Tantry, S. Weisman, A narrative review of the cardiovascular risks associated with concomitant aspirin and NSAID use, J. Thromb. Thrombolysis 47 (2019) 16–30.
[42] A.M. Qandil, Prodrugs of nonsteroidal anti-inflammatory drugs (NSAIDs), more than meets the eye: a critical review, Int. J. Mol. Sci. 13 (2012) 17244–17274.
[43] L. Huang, G.G. Mackenzie, Y. Sun, N. Ouyang, G. Xie, K. Vrankova, D. Komninou, B. Rigas, Chemotherapeutic properties of phospho-nonsteroidal anti-inflammatory drugs, a new class of anticancer compounds, Cancer Res. 71 (2011) 7617–7627.
[44] M. Chattopadhyay, R. Kodela, N. Nath, A. Barsegian, D. Boring, K. Kashfi, Hydrogen sulfide-releasing aspirin suppresses NF-κB signaling in estrogen receptor negative breast cancer cells in vitro and in vivo, Biochem. Pharmacol. 83 (2012) 723–732.
[45] N. Nath, M. Chattopadhyay, D.B. Rodes, A. Nazarenko, R. Kodela, K. Kashfi, Nitric oxide-releasing aspirin suppresses NF-κB signaling in estrogen receptor negative breast cancer cells in vitro and in vivo, Molecules 20 (2015) 12481–12499.
[46] C. Zhu, K.W. Cheng, N. Ouyang, L. Huang, Y. Sun, P. Constantinides, B. Rigas, Phosphosulindac (OXT-328) selectively targets breast cancer stem cells in vitro and in human breast cancer xenografts, Stem Cell. 30 (2012) 2065–2075.
[47] J.K. Wrobel, R. Power, M. Toborek, Biological activity of selenium: Revisited, IUBMB Life 68 (2016) 97–105.
[48] A.C. Ruberte, C. Sanmartin, C. Aydillo, A.K. Sharma, D. Plano, Development and therapeutic potential of selenazo compounds, J. Med. Chem. 63 (2020) 1473–1489.
[49] T. Lin, Z. Ding, N. Li, J. Xu, G. Luo, J. Liu, J. Shen, Seleno-cyclodextrin sensitises human breast cancer cells to TRAIL-induced apoptosis through DR5 induction and NF-κB suppression, Eur. J. Cancer 47 (2011) 1890–1907.
[50] P. Collery, Strategies for the development of selenium-based anticancer drugs, J. Trace Elem. Med. Biol. 50 (2018) 498–507.
[51] H.W. Tan, H.Y. Mo, A.T.Y. Lau, Y.M. Xu, Selenium species: current status and potentials in cancer prevention and therapy, Int. J. Mol. Sci. 20 (2018) 75.
[52] C. Sanmartín, D. Plano, A.K. Sharma, J.A. Palop, Selenium compounds, apoptosis and other types of cell death: an overview for cancer therapy, Int. J. Mol. Sci. 13 (2012) 9649–9672.
[53] I.L. Martins, J.P. Miranda, N.G. Oliveira, A.S. Fernandes, S. Gonçalves, A. M. Antunes, Synthesis and biological activity of 6-selenocaffeine: potential modulator of chemotherapeutic drugs in breast cancer cells, Molecules 18 (2013) 5251–5264.
[54] Y. Qi, X. Fu, Z. Xiong, H. Zhang, S.M. Hill, B.G. Rowan, Y. Dong, Methylseleninic acid enhances paclitaxel efficacy for the treatment of triple-negative breast cancer, PLoS One 7 (2012), e31539.
[55] X. Bi, N. Pohl, H. Dong, W. Yang, Selenium and sulindac are synergistic to inhibit intestinal tumorigenesis in Apc/p21 mice, J. Hematol. Oncol. 6 (2013) 8.
[56] R. Gowda, S.V. Madhunapantula, D. Desai, S. Amin, G.P. Robertson, Simultaneous targeting of COX-2 and AKT using selenocoxib-1-GSH to inhibit melanoma, Mol. Cancer Therapeut. 12 (2013) 3–15.
[57] D. Plano, D.N. Karelia, M.K. Pandey, J.E. Spallholz, S. Amin, A.K. Sharma, Design, synthesis, and biological evaluation of novel selenium (Se-NSAID) molecules as anticancer agents, J. Med. Chem. 59 (2016) 1946–1959.
[58] X. He, M. Zhong, S. Li, X. Li, Y. Li, Z. Li, Y. Gao, F. Ding, D. Wen, Y. Lei, Y. Zhang, Synthesis and biological evaluation of organoselenium (NSAIDs-SeCN and $SeCF_3$) derivatives as potential anticancer agents, Eur. J. Med. Chem. 208 (2020), 112864.
[59] X. He, Y. Nie, M. Zhong, S. Li, X. Li, Y. Guo, Z. Liu, Y. Gao, F. Ding, D. Wen, Y. Zhang, New organoselenides (NSAIDs-Se derivatives) as potential anticancer agents: synthesis, biological evaluation and in silico calculations, Eur. J. Med. Chem. 218 (2021), 113384.
[60] S. Ramos-Inza, A.C. Ruberte, C. Sanmartín, A.K. Sharma, D. Plano, NSAIDs: old acquaintance in the pipeline for cancer treatment and prevention—Structural modulation, mechanisms of action, and bright future, J. Med. Chem. 64 (2021) 16380–16421.
[61] D.N. Karelia, S. Kim, K.P. M, D. Plano, S. Amin, J. Lu, A.K. Sharma, Novel seleno-aspirinyl compound AS-10 induces apoptosis, G1 arrest of pancreatic ductal adenocarcinoma cells, inhibits their NF-κB signaling, and synergizes with gemcitabine cytotoxicity, Int. J. Mol. Sci. 22 (2021) 4966.
[62] C. Sanmartín, D. Plano, E. Domínguez, M. Font, A. Calvo, C. Prior, I. Encío, J. A. Palop, Synthesis and pharmacological screening of several aroyl and heteroaroyl selenylacetic acid derivatives as cytotoxic and antiproliferative agents, Molecules 14 (2009) 3313–3338.
[63] E. Domínguez-Álvarez, D. Plano, M. Font, A. Calvo, C. Prior, C. Jacob, J.A. Palop, C. Sanmartín, Synthesis and antiproliferative activity of novel selenoester derivatives, Eur. J. Med. Chem. 73 (2014) 153–166.
[64] N. Díaz-Argelich, I. Encío, D. Plano, A.P. Fernandes, J.A. Palop, C. Sanmartín, Novel methylselenoesters as antiproliferative agents, Molecules 22 (2017) 1288.
[65] S.O. Evans, P.F. Khairuddin, M.B. Jameson, Optimising selenium for modulation of cancer treatments, Anticancer Res. 37 (2017) 6497–6509.
[66] A.C. Ruberte, S. Ramos-Inza, C. Aydillo, I. Talavera, I. Encío, D. Plano, C. Sanmartín, Novel *N,N'*-disubstituted acylselenoureas as potential antioxidant and cytotoxic agents, Antioxidants 9 (2020) 55.
[67] B.A. Chabner, NCI-60 cell line screening: a radical departure in its time, J. Natl. Cancer Inst. 108 (2016) djv388.
[68] M.A. Marć, E. Domínguez-Álvarez, G. Latacz, A. Doroz-Plonka, C. Sanmartín, G. Spengler, J. Handzlik, Pharmaceutical and safety profile evaluation of novel selenocompounds with noteworthy anticancer activity, Pharmaceutics 14 (2022) 367.
[69] E.B. Asafu-Adjaye, P.J. Faustino, M.A. Tawakkul, L.W. Anderson, L.X. Yu, H. Kwon, D.A. Volpe, Validation and application of a stability-indicating HPLC method for the in vitro determination of gastric and intestinal stability of venlafaxine, J. Pharm. Biomed. Anal. 43 (2007) 1854–1859.
[70] W. Strober, Trypan blue exclusion test of cell viability, Curr. Protoc. Im. 111 (2015). A–3B.
[71] M. van Engeland, L.J. Nieland, F.C. Ramaekers, B. Schutte, C.P. Reutelingsperger, Annexin V-affinity assay: a review on an apoptosis detection system based on phosphatidylserine exposure, Cytometry 31 (1998) 1–9.
[72] N.C. Zembruski, V. Stache, W.E. Haefeli, J. Weiss, 7-Aminoactinomycin D for apoptosis staining in flow cytometry, Anal. Biochem. 429 (2012) 79–81.
[73] S. Kesavardhana, R.K.S. Malireddi, T.D. Kanneganti, Caspases in cell death, inflammation, and pyroptosis, Annu. Rev. Immunol. 38 (2020) 567–595.
[74] A. Boice, L. Bouchier-Hayes, Targeting apoptotic caspases in cancer, Biochim. Biophys. Acta Mol. Cell Res. 1867 (2020), 118688.
[75] R.U. Jänicke, MCF-7 breast carcinoma cells do not express caspase-3, Breast Cancer Res. Treat. 117 (2009) 219–221.
[76] Y. Naritomi, S. Terashita, S. Kimura, A. Suzuki, A. Kagayama, Y. Sugiyama, Prediction of human hepatic clearance from in vivo animal experiments and in vitro metabolic studies with liver microsomes from animals and humans, Drug Metab. Dispos. 29 (2001) 1316–1324.
[77] A. Daina, O. Michielin, V. Zoete, SwissADME: a free web tool to evaluate pharmacokinetics, drug-likeness and medicinal chemistry friendliness of small molecules, Sci. Rep. 7 (2017), 42717.
[78] T. Sander, J. Freyss, M. von Korff, J.R. Reich, C. Rufener, OSIRIS, an entirely in-house developed drug discovery informatics system, J. Chem. Inf. Model. 49 (2009) 232–246.
[79] S.K. Bharti, R. Roy, Quantitative H-1 NMR spectroscopy, Trac. Trends Anal. Chem. 35 (2012) 5–26.
[80] A. Pagoni, L. Marinelli, A. Di Stefano, M. Ciulla, H. Turkez, A. Mardinoglu, S. Vassiliou, I. Cacciatore, Novel anti-Alzheimer phenol-lipoyl hybrids: synthesis, physico-chemical characterization, and biological evaluation, Eur. J. Med. Chem. 186 (2020), 111880.
[81] R.H. Shoemaker, The NCI60 human tumour cell line anticancer drug screen, Nat. Rev. Cancer 6 (2006) 813–823.
[82] NCI-60 Screening methodology, Available on: https://dtp.cancer.gov/discovery_development/nci-60/methodology.htm.
[83] K.S. Louis, A.C. Siegel, Cell viability analysis using trypan blue: manual and automated methods, Methods Mol. Biol. 740 (2011) 7–12.